

Compressive strength of geopolymer concrete modified with nano-silica: Experimental and modeling investigations



Hemn Unis Ahmed ^{a,b,*}, Ahmed S. Mohammed ^a, Rabar H. Faraj ^{a,c},
Shaker M.A. Qaidi ^d, Azad A. Mohammed ^a

^a Civil Engineering Department, College of Engineering, University of Sulaimani, Sulaimani, Kurdistan Region, Iraq

^b Civil Engineering Department, Komar University of Science and Technology, Sulaimani, Kurdistan Region, Iraq

^c Civil Engineering Department, University of Halabja, Halabja, Kurdistan Region, Iraq

^d Civil Engineering Department, College of Engineering, University of Duhok, Duhok, Kurdistan Region, Iraq

ARTICLE INFO

Keywords:

Geopolymer concrete
Mix proportion
Nano-silica
Compressive strength
Modeling

ABSTRACT

Since nanotechnology can enhance the performance of materials, significant effort has been expended in recent years to incorporate nanoparticles (NPs) into geopolymer concrete (GPC) to improve performance and produce GPC with improved characteristics. Recent efforts have been made to incorporate various nanomaterials, most notably nano-silica (nS), into GPC to improve the composite's properties. Compressive strength (CS) is an important property of all concrete composites, including geopolymer concrete. Several mix proportion parameters and curing temperature and ages influence the CS of geopolymer concrete. As a result, developing a credible model for forecasting concrete CS is critical for saving time, energy, and money while also providing guidance for scheduling the construction process and removing formworks. This paper consists of three phases; in the first phase, a detailed review on the effect of adding nS on the CS of GPC was provided; then, in the second phase, a large amount of mixed design data were extracted from literature studies to create five different models including artificial neural network, M5P-tree, linear regression, nonlinear regression, and multi logistic regression models for forecasting the CS of GPC incorporated nS. Finally, the developed models were validated in the last phase by carrying out experimental laboratory works. Results revealed that the addition of nS improves the CS of GPC, and the ANN model estimated the CS of GPC incorporated nS more accurately than the other models. On the other hand, the alkaline solution to binder ratio, molarity, NaOH content, curing temperature, and ages were those parameters that significantly influenced the CS of GPC incorporated nS.

Abbreviations: C-A-S-H, calcium-alumino-silicate-hydrate; GPC, Geopolymer concrete; nS, Nano-silica; CS, Compressive strength; R², Coefficient of determination; RMSE, Root mean squared error; MAE, Mean absolute error; SI, Scatter index; OBJ, Objective function value; LR, Linear regression; NLR, Nonlinear regression; MLR, Multi-logistic regression; ANN, Artificial neural network; M5P, M5P-tree; l/b, Alkaline solution to binder ratio; SH, Sodium hydroxide; SS, Sodium silicate; SS/SH, Sodium silicate to sodium hydroxide ratio; M, Molarity of sodium hydroxide; FA, Fine aggregate; CA, Coarse aggregate; T, Curing temperature; A, Geopolymer concrete specimens ages; B, Binder content; nm, Nanometer; NPs, Nanoparticles; nC, Nano-clay; nA, Nano-alumina; nM, Nano-metakaolin; nT, Nano-titanium; C-S-H, Calcium-silicate-hydrate; FTIR, Fourier transform infrared; GGBFS, Ground granulated blast furnace slag; CNT, Carbon nanotube; N-A-S-H, sodium-alumino-silicate-hydrate; OPC, Ordinary portland cement; SEM, Scanning electron microscope; SF, Silica-fume; XRD, X-ray diffraction.

* Corresponding author at: Civil Engineering Department, College of Engineering, University of Sulaimani, Sulaimani, Kurdistan Region, Iraq.

E-mail addresses: henn.ahmed@univsul.edu.iq, hemnunis@yahoo.com (H.U. Ahmed).

<https://doi.org/10.1016/j.cscm.2022.e01036>

Received 7 December 2021; Received in revised form 12 March 2022; Accepted 26 March 2022

Available online 28 March 2022

2214-5095/© 2022 The Author(s). Published by Elsevier Ltd. This is an open access article under the CC BY-NC-ND license (<http://creativecommons.org/licenses/by-nc-nd/4.0/>).

1. Introduction

Concrete, after water, is the second most useful material for the construction industry [1,2]. Every year, 25 billion tons of concrete are produced worldwide, acquiring 2.6 billion tons of cement, which will increase by 25% over the next ten years [3]. Cement production has a negative impact on the environment because one ton of cement emits one ton of CO₂ into the atmosphere, alarming the ecology [4]. However, cement-based concrete remains the most widely used material in the global building industry [5]. Therefore, all nations have become mandatory to consider CO₂ emission regulations and reductions [6]. As a result, extensive research has been conducted to develop a new material that can be used as an alternative to Portland cement [7]; among them, geopolymmer technology was developed in France by Professor Davidovits [8]. Due to the high consumption of waste materials in mixed proportions, GPC emits approximately 70% less green gas than conventional concrete [9].

Geopolymers are an inorganic alumino-silicate polymer family produced through alkaline activation of various aluminosilicate virgin or waste materials rich in silicon and aluminum [10,11]. The mixed proportions of the GPC consist of aluminosilicate source binder materials, fine and coarse aggregates, alkaline solutions, and water [12]. The polymerization process consists of four main steps: dissolution, condensation, polycondensation, and crystallization of the gels, between the alkaline solutions and source binder materials, produced solid concrete, like traditional concrete composites [13,14]. Sodium hydroxide and sodium silicate are commonly used alkaline activators to create geopolymers. These two activators were produced commercially, so they have adverse effects on environmental issues; therefore, it is essential to use activators that were made cleanly and environmentally friendly such as a mixture of NaOH and glass waste and a mixture of olive biomass ash and water [15]. In addition, de Azevedo et al. [16] successfully used lapidating waste of flat glasses as a precursor in geopolymers materials to manufacture ecological ceramic roof tiles with satisfied properties; furthermore, the use of this waste opens up a new way of using this material, which is typically discarded in landfills, which is an environmental benefit of its application and can lead to a reduction in the economic costs of this process [17].

The molarity of NaOH, the ratio of Na₂SiO₃/NaOH, the curing regime and ages, the water to solids ratio, the alkaline solution to binder ratio, the elemental composition and type of source binder materials, the ratio of Si to Al in the geopolymers system, the mixing time and rest period, the superplasticizer dosage and extra water contents, and the coarse and fine aggregate contents were all factors that influenced the properties and performances of GPC [18].

Nanotechnology and nanomaterials have recently sparked a lot of interest worldwide due to their high performance in a variety of fields. The construction industry, for example, can benefit from nanotechnology by using nanoparticle (NP) materials in the concrete industry to create high-performance and innovative concrete composites. Nanotechnology is the ability to monitor and restructure matter at the atomic and molecular levels in the range of 1–100 nm, as well as the contribution to the distinct properties and phenomena at that size that are equivalent to those associated with individual atoms and molecules or bulk behavior [19,20]. The primary reason for incorporating NPs into all types of concrete composites, including GPC, is to improve the microstructural properties of the concrete composite. As a result, all other composite properties, such as mechanical and physical properties, as well as the durability of concrete composites, would be enhanced [21]. In the literature, a wide range of NPs like nano-silica (nS) [22], nano-clay (nC) [23], nano-alumina (nA) [24], carbon nanotubes (CNT) [25], nano-metakaolin (nM) [26], nano-titanium (nT) [27] were consumed to improve various properties of the geopolymers composites, with nS being the most frequent [21]. Since nano-silica was the most frequently used material among all types of NPs, this study focused on developing various models for estimating the CS of GPC composites incorporating nS.

All concrete composites, including GPC, need to be strong when compressed. The CS gives a general idea of how good the concrete is [28]. However, the concrete's CS at 28 days is very important for building structures. As a result, getting a good model for figuring out the CS of concrete is very important for changing or verifying the concrete mix proportions [29]. Many factors affect the CS of GPC, which leads to a wide range of compressive strength results. This makes it hard to figure out the CS, which is a problem for both scholars and engineers. As a result, new numerical and mathematical models are needed to understand this issue [30] better. Machine learning methods have been used in the literature to model different aspects of concretes, such as the CS of green concrete [31], the CS of nS-modified self-compacting concrete [32], the CS of fly ash-based GPC composites [33], the CS of fly ash-based geopolymers mortar [34], and so on.

The current study is divided into three phases: the first phase provides a detailed review of the effect of adding nS on the CS of GPC; the second phase extracts a large amount of mixed design data from literature studies to create five different models for forecasting the CS of GPC incorporated nS, including artificial neural network, M5P-tree, linear regression, nonlinear regression, and multi logistic regression models. Finally, the developed models were validated in the final phase through experimental laboratory work.

2. Methodology

This study is divided into three sections: review, modeling, and experimental work. To gather information about geopolymers concrete incorporated NPs, an extensive search of several databases, including Research Gate, Science Direct, Google Scholar, Scopus, and the Web of Science, was conducted. It was discovered that a wide variety of NPs, including nS, nC, nA, CNT, nM, and nT, were used to improve various properties of GPC composites, with nS being the most commonly used. As a result, in this study, the authors use articles that used nS to improve various properties of GPC composites to create the models. However, all GPC papers containing NPs were taken into account for the review process. In the modeling process, eleven input parameters were used, limiting the authors' ability to utilize a more significant number of data in the created models. The gathered datasets (207) were statistically analyzed and classified into three groups. The models (LR, NLR, MLR, ANN, and M5P) were built using the larger group, including 135 datasets. The

Table 1

Summary of the constituents of geopolymers concrete mixes reported in the literature.

Ref.	l/b	B (kg/m ³)	FA (kg/m ³)	CA (kg/m ³)	SH (kg/m ³)	SS (kg/m ³)	M	SS/SH	nS (kg/m ³)	T (°C)	A (days)	CS (MPa)
[22]	0.45	486–490	490	1470	73	154	12	2	0–3.675	31.5	3_28	8.95–62.8
[24]	0.45	362.8	990	810	122.4	40.8	4	0.33	0–10.88	25	7–120	35.5–61.8
[26]	0.45	500–460	790	907	62.5	187.5	12	2.33	0–40	28	7_28	29–48
[35]	0.45	500	575	1150	64.3	160.7	14	2.5	0–15	70	30	51.63–42.71
[36]	0.4	440	723	1085	64	112	12	1.75	0–26.4	28–60	3_28	21.7–46.43
[37]	0.45	393–414	692–684	1240–1233	46.6–44.2	139.7–132.6	4	3	0–20.7	23	28–60	52–76.5
[38]	0.6	450	500	970–1150	135	135	10	1	0–13.5	25	7_90	18.6–47.3
[39]	0.45	380.689	554.4	1295	48.945	122.364	8_16	2.5	0–5.71	60	28	38.1
[40]	0.52	370–400	650	1206	60	150	14	2.5	0–30	60	1_28	4.7–45
[41]	0.6	300	800	1200	85	95	12	1.1	0–9	25	7_28	18.9–45.9
[42]	0.5	339–350	720	1305	43.5–45	108.9–112.5	16	2.5	0–21	60	7_28	3.2–24.4
[43]	0.6	450	500	1036–1150	108	162	12	1.5	0–9	60	28	31.6–42.6
[44]	0.45	497	560	1120	159.75	63.9	12	0.4	0–49.7	60	28	24–35
[45]	0.5	450	750	1000	75	150	12	2	0–13.5	25	7_28	21.9–50.4
[46]	0.4	394.29	554.4	1293.6	45.06	112.64	12	2.5	0–3.94	24	28	44.3–48.6
[47]	0.45	450–500	825	825	18.17–28.57	144.65–160.75	10_16	2.5	0–10	60	7_90	41.1–81.3
[48]	0.52	370–400	620–650	1152–1206	60	150	14	2.5	0–60	24	3–180	4.3–61.2
[49]	0.45	405.8–413.8	888	945	53.2	133	12	2.5	0–8.3	29	28–90	37.1–52.3
[50]	0.52	370–400	620–650	1152–1206	60	150	14	2.5	0–60	60	0.5–28	4.9–45.1
Current study	0.5	450	590.92–609.83	1065.72–1099.83	64.3	160.7	12	2.5	0–18	23	28	29.8–35.9
Min.	0.4	300	490	810	18.17	40.8	4	0.33	0	23	0.5	3.2
Max.	0.6	500	990	1470	159.75	187.5	16	3	60	70	180	81.3
St.Div.	0.1	51.9	135.3	183.3	33.9	35.6	3.3	0.8	14.6	17.4	31.8	17.5

Notes: l/b=alkaline solution to binder ratio, B=binder content (kg/m³), FA=fine aggregate content (kg/m³), CA=coarse aggregate content (kg/m³), SH=sodium hydroxide content (kg/m³), SS=sodium silicate content (kg/m³), M=molarity (M), SS/SH=ratio of sodium silicate to sodium hydroxide, nS=nano-silica content (kg/m³), T = curing temperature (°C), A=age (days), and CS=tested compressive strength (MPa).

second group is made up of 36 datasets that were used to test the created models, and the final group is made up of 36 datasets that were consumed to validate the suggested models [29,32]. Table 1 summarizes the dataset ranges, including all significant parameters and the observed CS of the GPC incorporated nS. While Table 2 shows some statistical characteristics of the collected datasets. The developed models were evaluated using statistical criteria such as R^2 , RMSE, MAE, SI, and OBJ to determine the most reliable and accurate model. Finally, five different GPC mixtures with varying nS concentrations were prepared; the prepared specimens were tested after 28 days. The proposed models were validated using test results with mixed proportions. Additional details about this work's methodology are shortened in a flow chart, as illustrated in Fig. 1.

3. Reviewing phase

The literature examined the CS property of various geopolymer composite types incorporating dissimilar NPs in detail. Fig. 2 illustrates the effect of NPs incorporation on the CS of geopolymer concrete at a curing age of 28 days. In general, the figures demonstrate that adding NPs increases the CS of geopolymer composites up to a certain NPs dosage.

The fresh, mechanical, and microstructural properties of geopolymer concrete at various volume fractions of nS have been investigated. They discovered that all mixtures containing nS had greater compressive strength than a virgin mixture devoid of nS. At 28 days ambient curing temperature, the highest CS was obtained at 1.5% of nS dosage, which increased the CS by 11% compared to the control mix. The increased strength is attributed to the filling of nanopores within the geopolymer concrete matrix with silica nanoparticles, which densifies and compacts the matrix. Additionally, the chemical composition of the nS, which is high in silica, accelerates the geopolymer reactions and strengthens the geopolymer binder, thereby increasing the specimens' strength. Additionally, they prefer a concentration of nS of 1.5% as the optimal concentration for improving the compressive strength; above that concentration, the CS slightly decreases due to the overflowing availability of unreacted nS particles in the matrix, and the excess amount of nS causes agglomerations between the nS particles, preventing silica dissolution and resulting in the formation of voids, lowering the compressive strength of the geopolymer concrete [22]. Similarly, [38,39,44,45,47,49] discovered that adding nS improves the CS of geopolymer concrete. Additionally, Nuaklong et al. [43] discovered that incorporating nS improves the CS of geopolymer concrete by up to 2%; and then, a decrease in the CS was observed above that dosage. Furthermore, Angelin Lincy and Velkennedy [46] observed that the addition of nS enhanced the CS of geopolymer concrete up to 0.5% of nS dosage, and then a reduction in the CS was recorded. However, Ibrahim et al. [50] and Janaki et al. [51] revealed that the CS of geopolymer concrete increased as the dosage of NPs increased up to 5% and then decreased. For instance, the CS was increased by 1.5%, 13.6%, and 1.3% at 2%, 5%, and 10% of CNT, respectively, at the age of 28 days [51], while this increment in the CS was 0%, 8.2%, 23.3%, and 19.8% at 1%, 2.5%, 5%, and 7.5% of nS, correspondingly, at the age of 28 days [50]. Further, the CS enhancement of about 81% and 57% was recorded when 0.02% of CNTs added to the geopolymer concrete mixtures among geopolymer concrete mixtures with various CNTs inclusion compared to the control mixes at the curing age of 28 and 60 days, respectively [25]. This strength enhancement was argued that the CNTs act as bridges for reducing micro and macro cracks propagation [52]. The alkaline liquid influences CNTs dispersion as the CNTs were surfactant by sodium hydroxide, letting them produce well-dispersed CNTs and de-bundle within the geopolymer concrete matrix [53,54]. In the same manner, Kotop et al. [25] reported that the largest CS improvement was 99% and 70% at 28 and 60 days, respectively, for the geopolymer concrete mixtures incorporating a hybrid of 2.5% of nS and 0.01% of CNTs, as compared to the control geopolymer concrete mixture without any NPs inclusion.

In the same context, experimental work has been carried out by Khater [55] to investigate the physio-mechanical properties of nS effects on the geopolymer concrete. Various volume fractions of nS range from (0–8%) were used. The output of this research reported that the inclusion of nS improves the CS of the geopolymer concrete up to 3%. In contrast, a further increase in nS dosage decreases the CS due to the accumulations of the nS particles. The maximum CS was 36 MPa for 3% of nS content compared to the 25 MPa of the control mix without incorporating nS. Also, this optimum dosage (3%) of nS was reported in other studies [37,41]. However, Rabiaa et al. [26] observed that 4% of nS was optimum content among (0–8%) of nS dosages. Behfarnia and Rostami [37] reported that substituting 3% nS enhances the 28-day CS by 12%. Meanwhile, beyond this dosage, a reduction in the CS was observed. This result may be argued to the fact that nS participate in the pozzolanic reaction to produce extra C-S-H gel and fill the pores inside the matrix in

Table 2
Summary of statistical analysis of input model parameters.

Model parameters	No. of data	Average	Median	St.Div.	Min.	Max.	Variance	Skewness	Kurtosis
l/b	207	0.49	0.5	0.1	0.4	0.6	0.0	0.66	-0.25
B (kg/m ³)	207	417.22	400	51.9	300	500	2689.5	0.11	-0.81
FA (kg/m ³)	207	680.96	650	135.3	490	990	18,294.6	0.63	-0.10
CA (kg/m ³)	207	1113.85	1170	183.3	810	1470	33,580.8	-0.20	-0.72
SH (kg/m ³)	207	71.36	60	33.9	18.17	159.75	1150.6	1.10	0.49
SS (kg/m ³)	207	134.43	150	35.6	40.8	187.5	1268.2	-1.43	1.56
M	207	11.97	12	3.3	4	16	11.1	-1.43	1.31
SS/SH	207	2.06	2.5	0.8	0.33	3	0.6	-1.26	0.22
nS (kg/m ³)	207	11.65	8	14.6	0	60	211.8	1.85	3.09
T (°C)	207	42.06	31.5	17.4	23	70	304.0	0.12	-1.93
A (days)	207	28.30	28	31.8	0.5	180	1012.9	2.37	6.96
CS (MPa)	207	36.18	35.8	17.5	3.2	81.3	307.0	0.15	-0.75

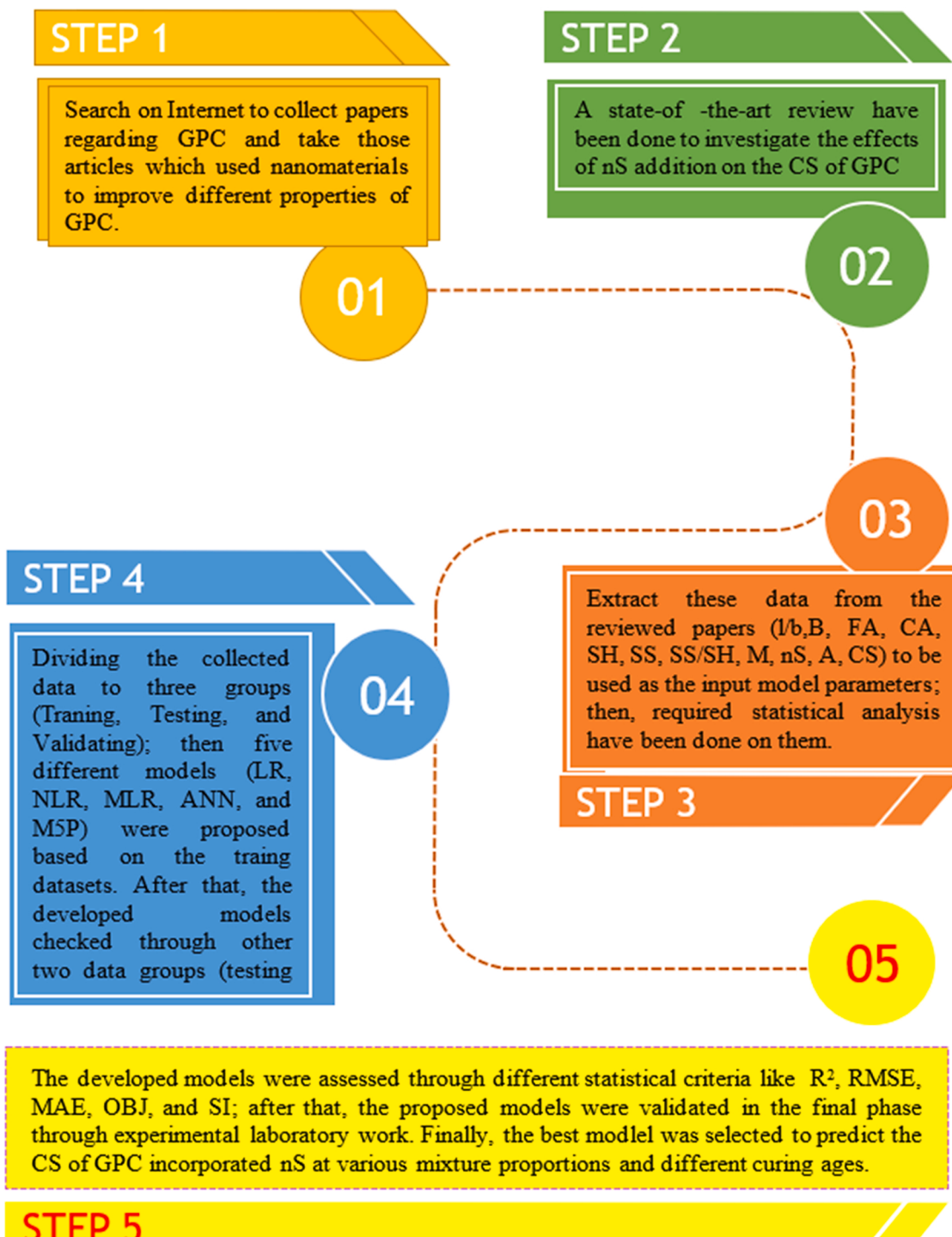


Fig. 1. The flow chart diagram process followed in this study.

the range of nanoscale, while the reduction in strength was attributed to agglomerations of nS particles in the geopolymer concrete mixture followed by the formation of voids in the concrete matrix [37].

Moreover, another research study was carried out on the influence of nS on the microstructure and strength of natural pozzolan-based geopolymer concrete, and they used 0, 1%, 2.5%, 5%, and 7.5% of NS. They observed that the nS increases the CS of the geopolymer concrete, and the highest value (about 18%) is for the specimens with 5% of nS dosage. In contrast, the minimum values

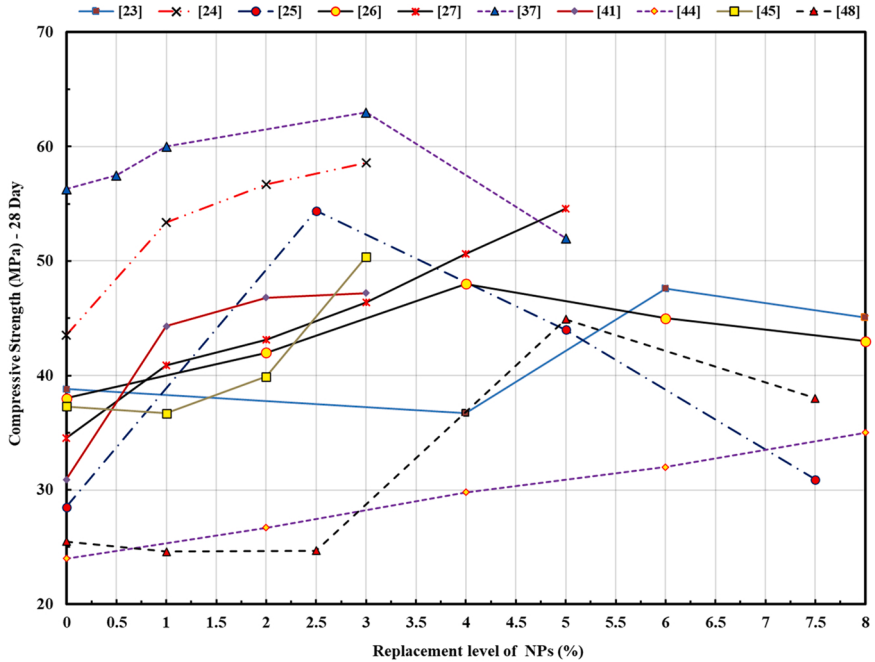


Fig. 2. CS versus NPs content of different geopolymers composites and NP types – 28 Days.

were measured in the reference geopolymers concrete mixture without any nS content [40]. Similarly, the inclusion of nS particles improves the structural performance of the geopolymers concrete [36]. On the other hand, fewer studies [27,42] have been conducted in the literature to investigate the effects of nT on the various properties of geopolymers concrete. Sastry et al. [27] claimed that CS was significantly improved with nT increment. For instance, the CS was increased by 21%, 23%, 31%, 33%, and 36% at the age of 7 days and 16%, 20%, 26%, 32%, and 37% at the age of 28 days, when the dosage of nT was 1%, 2%, 3%, 4% and 5% dosage, correspondingly, in comparison to the corresponding concrete mixtures without any nT. Moreover, the outcome of the other experimental research work revealed that adding 1% of nT improves CS by 32.96% and 46.65% at 7 and 28 days, respectively, compared to the control mixture without any nT content [42].

Few researchers dealt with the influences of adding nano-clay (nC) and nano-metakaolin (nM) on the strength and durability properties of geopolymers concrete mixtures [23,26,41]. A research study was conducted to investigate the effects of nC additions on the durability properties of geopolymers concrete composites. The outputs of this study indicated that the CS was increased with the increment of nC contents. The CS of 3% content of nC geopolymers concrete specimens improved by 1.39 and 1.44 times compared to

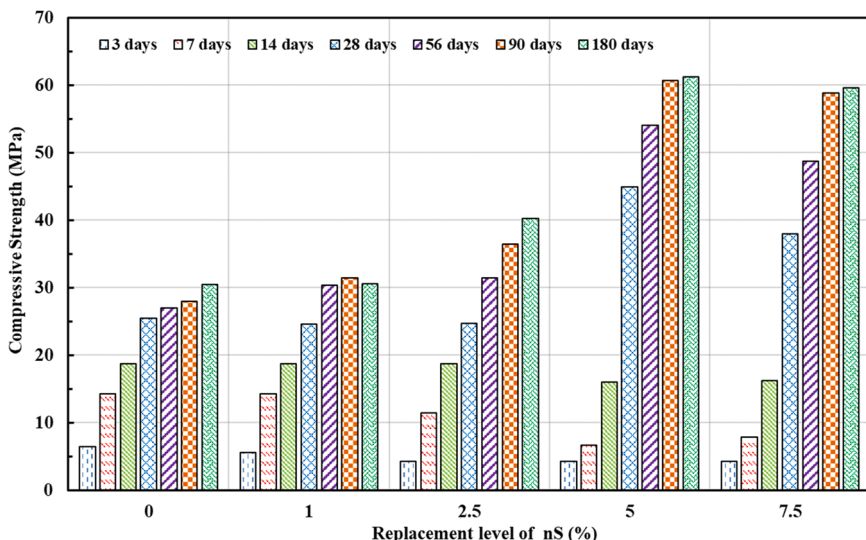


Fig. 3. CS of geopolymers concrete incorporating different dosages of nS at different curing ages.

the reference sample at the age of 7 and 28 days, respectively [41]. Similarly, Ravitheja and Kumar [23] reported that the inclusion of nC improves the CS of the geopolymer concrete mixtures up to 6% nC; beyond that dosage, a slight reduction in the strength was recorded. Also, they showed that the maximum CS took place at the 6% of nC content, which is 32, 37.5, and 47.5 MPa, compared to the control geopolymer concrete mixture, which is 26, 32, and 39 MPa, at the age of 3, 7 and 28 days, correspondingly.

Moreover, an experimental research study has been carried out to investigate the effect of nM on the properties of geopolymer concrete. They used 0%, 2%, 4%, 6%, and 8% of nM to improve the characteristics of the geopolymer concrete. CS was improved about 12% and 16% at 6% nM in the age of 7 and 28 days, respectively, compared to the control mixture, whereas, after 6% of nM slight decrease in the CS was reported [26]. This CS enhancement is attributed to the fact that the interfacial transition zone improved with the presence of the required content of nM, which reduces the amount of porosity and increases the compactness of the specimens. Consequently, CS was improved. However, the reduction of CS beyond 6% dosage of nM could be argued that agglomerations among NPs of metakaolin were taken place, which leads to producing pores, which could also be attributed to the incomplete hydration reactions [26]. Furthermore, Shahrajabian and Behfarnia [24] observed that the addition of nC and nA led to a slight decrease in the CS of GGBFS-based geopolymer concrete at the age of 7 and 28 days, while, at the later ages of 90 and 120 days, improvement in the CS was recorded. Also, they observed that the inclusion of nS in the geopolymer concrete mixtures improves the CS at 7, 28, 90, and 120 days.

Lastly, experimental research work has been carried out by Ibrahim et al. [48] to investigate the effect of nS inclusions on the engineering characteristics and microstructure of alkali-activated concrete. They reported that the addition of nS has a slightly negative effect on the CS of the concrete mixtures at the age of 3, 7, and 14 days, and then at the later ages of 28, 56, 90, and 180 days, CS was improved up to 5% of nS content, after that the CS was slightly declined as depicted in Fig. 3 which is adapted from [48]. For example, at the age of 7-day, the CS was decreased by 0%, 19.7%, 53.5%, and 45% at 1%, 2.5%, 5%, and 7.5% of nS dosages, correspondingly. This result was argued to be the decline in the PH of the concrete mixture due to the inclusion of colloidal nS. While, at the age of 90-day, CS was increased by 12.1%, 30%, 117%, and 110% at 1%, 2.5%, 5%, and 7.5% of nS inclusion, respectively. This result was attributed to the fact that at the later ages of the geopolymer concrete mixture, the aluminosilicate species of the source binder materials contributed to the gel formation and, subsequently, the poly-condensation to form an increasingly larger three-dimensional network, particularly due to the availability of reactive nS.

4. Experimental phase

4.1. Materials

This study was carried out by defining five mix designs: four with varying amounts of nano-silica (1%, 2%, 3%, and 4%) and a control design. Table 3 shows the compositions of these mixes in detail. This study used ground granulated blast furnace slag (GGBFS) with a specific gravity of 2.9 and a specific surface (Blaine) of 5800 cm²/g as the primary source binder materials. The chemical composition and the SEM of the GGBFS are shown in Table 4 and Fig. 4a, respectively. Further, a constant amount of silica fume (SF) with a specific gravity of 2.25 was used as the GGBFS replacement to prepare the geopolymer concrete mixtures. The chemical composition and the SEM of the SF are shown in Table 4 and Fig. 4b, respectively. In addition, nano-silica (nS) with the size of 30 nm, bulk density 0.18 g/cm³, purity of 99.5%, and the surface area of 185 ± 20 m²/g are used. The XRD and FTIR of the nS are presented in Fig. 5a, and b. the nS replaced the GGBFS by four different percentages of 1%, 2%, 3%, and 4%.

Sodium hydroxide and sodium silicate mixtures are used as alkaline solutions. The sodium hydroxide with a purity of 98% is dissolved in water to prepare the required molarity, and the sodium silicate solution consisting of 37.5% SiO₂, 16.5% Na₂O, and 46% H₂O is consumed. The alkaline solution to the total binder ratio was fixed at 0.5, and sodium silicate to sodium hydroxide was 2.5.

Natural fine and crushed coarse aggregates with specific gravities of 2.77 and 2.69 are utilized, respectively. The gradations of the fine and coarse aggregates are shown in Fig. 6a and b, correspondingly.

The chemical and mineralogical compositions of nano-silica were investigated using X-ray diffraction (Angstrom Advanced ADX-2700, ADX-2700 SSC). The test patterns were generated using (Cu-K α radiation, $\lambda = 1.55046 \text{ \AA}$) on an Angstrom Advanced XRD platform ADX-2700 diffractometer (USA) equipped with a graphite monochromator. The test was conducted at a 40 kV accelerating voltage, 30 mA, and 0.050 per phase-scanning system with a 5 s/phase step and an acquisition time of 2 thetas in the angle range of 0–70°.

The infrared spectrum of absorption of the nano-silica in powder condition was identified and characterized using FTIR. The spectral resolution was set to 1/cm, and the number of scans was set to 32, with the optical frequency space selected between 400 and

Table 3
GPC mixtures proportions.

Mix proportions (kg/m ³)								
Mix ID	GGBFS	SF	nS	SH	SS	Gravel	Sand	nS%
G1	400	50	0	64.3	160.7	1099.83	609.83	0
G2	395.5	50	4.5	64.3	160.7	1091.30	605.10	1
G3	391	50	9	64.3	160.7	1082.78	600.37	2
G4	386.5	50	13.5	64.3	160.7	1074.25	595.64	3
G5	382	50	18	64.3	160.7	1065.72	590.92	4

Table 4
Chemical composition of GGBFS and SF.

Elements	GGBFS	SF
	wt%	wt%
Na ₂ O	1.7800	—
MgO	6.675	0.33
Al ₂ O ₃	11.641	—
SiO ₂	38.159	92.4
SO ₃	1.93	—
K ₂ O	0.8045	—
CaO	30.966	0.143
TiO ₂	1.51	—
Fe ₂ O ₃	1.591	0.13
MnO	2.295	—
Ba	0.517	—
Sr	0.07	—
Cu	0.07	—
LOI	2	7

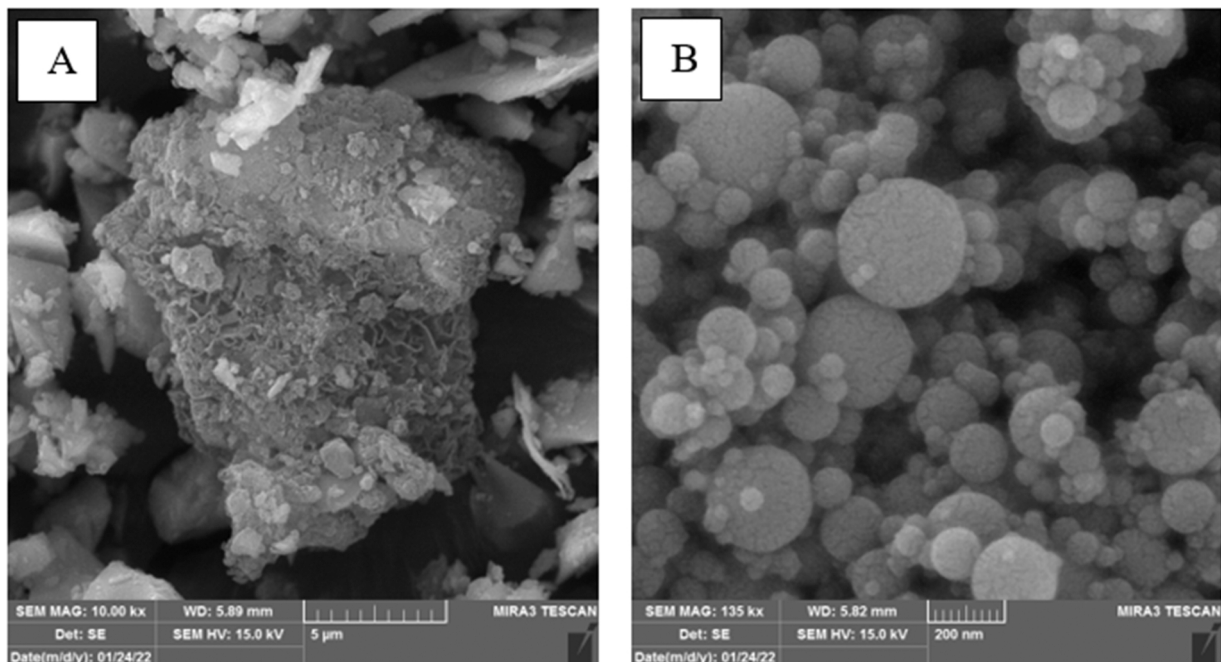


Fig. 4. SEM images; (a): GGBFS; (b): SF.

1/cm 4000 1/cm.

The SEM quanta 400 from FEI Company, a high-quality field emission gun scanning electron microscope suitable for imaging and identifying nano-scale particles, was used in this study. The samples were collected by first applying conductive tape to the stamp surface and then placing the samples (GGBFS and SF) on it. The specimen holder was inserted into the corresponding hole on the sample holder mount. In fine-grained powder, the GGBFS and SF are tested.

4.2. Mixing, specimens preparation, and testing

Firstly, to prepare the geopolymers concrete mixtures, the fine and coarse aggregates were dry mixed in a concrete mixer for about 30 s, then, in the second stage, a blend of GGBFS, SF, and NS was added to the mixer and further mixed with aggregates for about 60 s. After that, in the third stage, the alkaline solution, which was prepared 24 hr before mixing added to the concrete mixer slowly, followed by 180 s of mixing. Following the mixing step, the slump test was used to determine the workability of the fresh geopolymers concrete based on the ASTM C143.

When the fresh concrete was put into molds, a vibrating table was used to make it even denser and get rid of air bubbles. After 24 hr, the specimens were removed from the mold and cured in the lab at 23 ± 2 °C until they were ready for the test. Finally, three

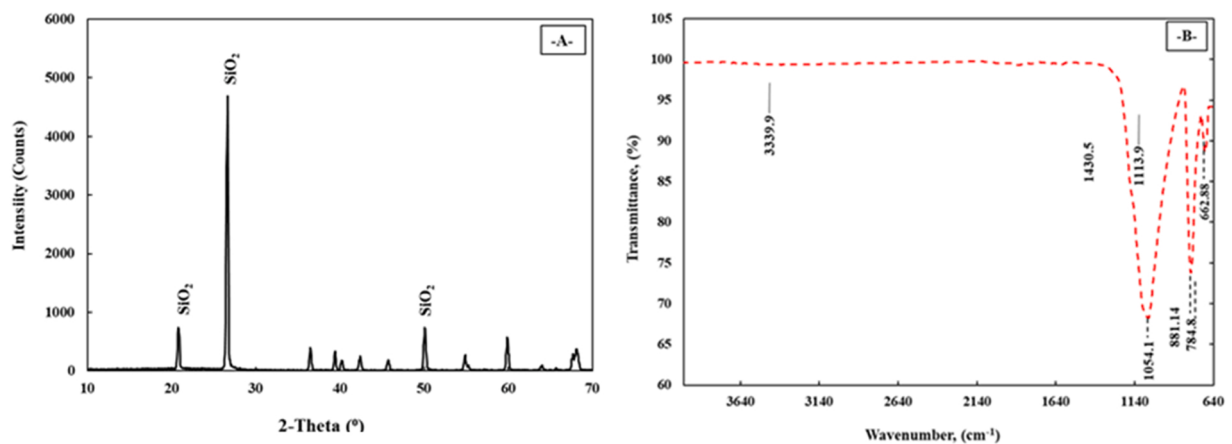


Fig. 5. (a): XRD pattern of nS; (b): FTIR spectra of nS.

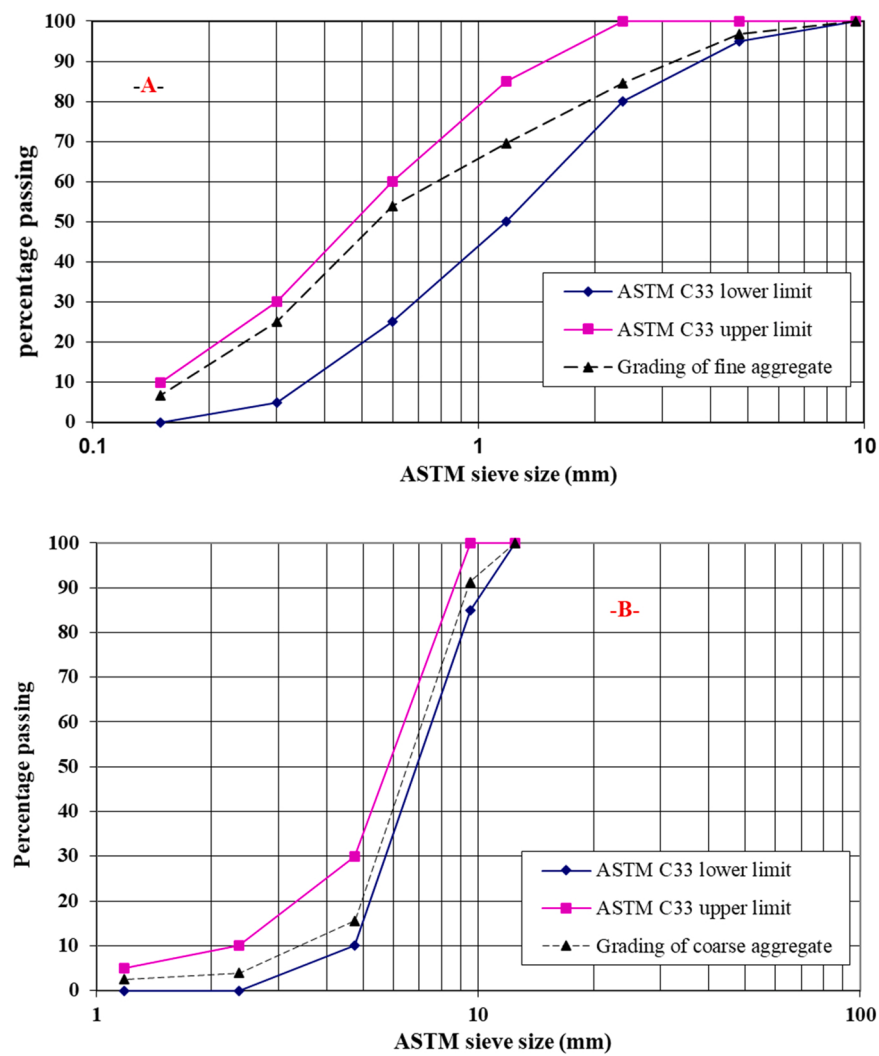


Fig. 6. Gradation of aggregates; (a): fine aggregate; (b): coarse aggregate.

100 * 200 mm cylinder specimens were examined under compression at the ages of 3, 7, and 28 days to assess the compressive strength of geopolymers concrete, according to ASTM C39. Additional details about the experimental laboratory works are presented in Fig. 7.

5. Modeling phase

5.1. Statistical assessment

Sufficient information about each variable input model parameter is provided in the following sections through 5.1.1 to 5.1.12. A histogram was plotted to discover and show the underlying frequency distribution (shape) of a set of continuous material properties datasets. This allows the inspection of the data for its underlying distribution (e.g., normal distribution), outliers, and skewness [34]. In addition, the statistical criteria such as standard deviation, variance, skewness, and kurtosis were determined to illustrate the distribution of each variable with compressive strength. The kurtosis is a statistical indicator that explains how heavily the tails of a distribution of a set of data differ from the tails of the normal distribution. In addition, the kurtosis finds the heaviness of the distribution tails, while skewness measures the symmetry of the distribution. On the other hand, the skewness could be quantified as an impersonation of the range to which a given distribution differs from a normal distribution. For instance, the skew of zero value was measured for normal distribution, while the right skew is an indication of the lognormal distribution; further, the variance informed of the degree of spread in the dataset, the greater the spread of the data, the greater the variance is about the mean [33].

5.1.1. The alkaline solution to binder ratio (l/b)

The alkaline solution is the total amount of alkaline activator (both sodium silicate solution and sodium hydroxide solution with required molarities) which were used to activate the source binder materials. Based on the collected datasets, the ratio of l/b of the GPC mixtures modified with nS was in the range of 0.4–0.6, with the average and standard deviations of 0.49 and 0.05, respectively. Also, regarding other statistical analyses, it was found that the variance was 0.002, skewness was 0.66, and the kurtosis was – 0.25. Fig. 8 depicts the relationship between CS and l/b with histograms of GPC mixtures incorporated nS.

5.1.2. Binder content (B)

Fly ash, GGBFS, MK, SF, RHA, and NP are those ashes that scholars used as source binder materials to produce GPC composites. The



Fig. 7. Experimental laboratory procedure works.

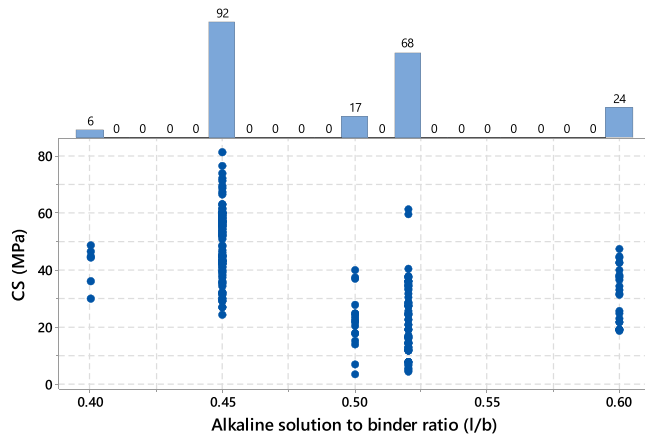


Fig. 8. Marginal plot between CS and l/b ratio of GPC mixtures incorporated nS.

ranges of these binders were between 300 and 500 kg/m³, with the average and standard deviations of 417 kg/m³ and 51.8 kg/m³, correspondingly. At the same time, other statistical assessment tools like variance, skewness, and kurtosis were 2689, 0.11, and – 0.81, respectively, for the collected datasets. Fig. 9 illustrates the CS and b content variation and frequencies of the gathered data of GPC mixtures incorporated nS.

5.1.3. Fine aggregate content (FA)

Natural and crushed sands were used as the FA in GPC mixtures like traditional concrete mixtures. The FA should be satisfied with the requirements of ASTM C33 standards. According to gathered datasets from the literature article, it was found that the range of FA was between 490 and 990 kg/m³, with an average of 681 kg/m³ and standard deviations of 135.2 kg/m³. More information regarding other statistical assessment tools can be found in Fig. 10.

5.1.4. Coarse aggregate content (CA)

Natural, crushed, and recycled aggregates are those forms of aggregates that were used as the CA in geopolymer concrete mixtures, just like conventional concrete mixtures. Same as FA, the CA should have all the properties which are required by ASTM C33 standards. Regarding the ranges of CA, it was concluded that the contents of CA in past research varied between 810 and 1470 kg/m³ with an average of 1113.8 kg/m³ and standard deviations of 183.2 kg/m³. On the other hand, the variance, skewness, and kurtosis were 33,580, – 0.19, – 0.71, respectively. Also, the correlations between the CS of tested datasets and the CA contents can be found in Fig. 11.

5.1.5. NaOH content (SH)

Pellets and flakes are two forms of SH in a solid-state with a purity above 97%. This material is mixed with the required amount of water to prepare a solution of SH with the required molarity. In this study, according to the collected datasets, the amount of SH in a 1 m³ of GPC mixture incorporated nS was in the range between 18.1 and 159.7 kg/m³, with an average of 71.3 kg/m³ and a standard deviation of 33.9 kg/m³. Extra information about other statistical assessment criteria and correlations between the CS and SH content

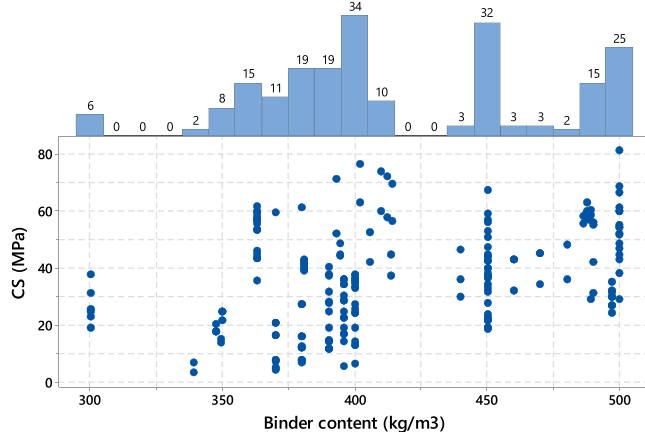


Fig. 9. Marginal plot between CS and binder content of GPC mixtures incorporated nS.

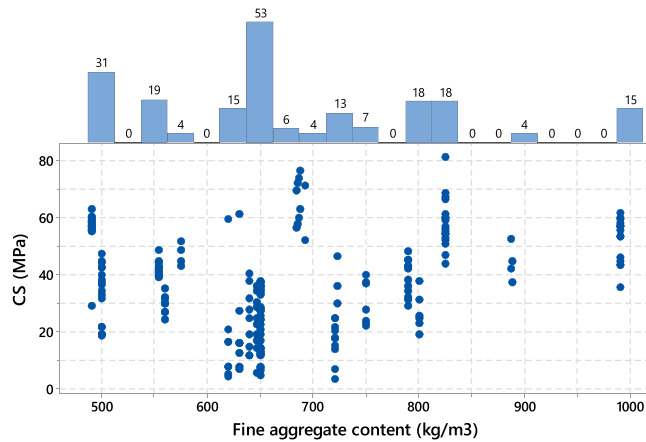


Fig. 10. Marginal plot between CS and FA content of GPC mixtures incorporated nS.

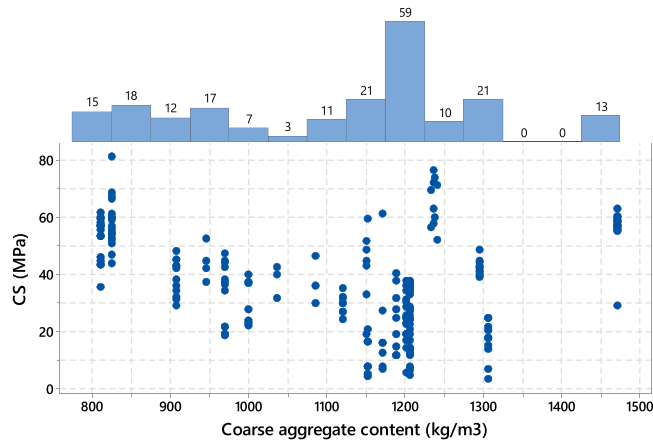


Fig. 11. Marginal plot between CS and CA content of GPC mixtures incorporated nS.

can be found in Fig. 12.

5.1.6. Na_2SiO_3 content (SS)

Water glass or sodium silicate is present in a liquid form which mainly consists of Na_2O , SiO_2 , and H_2O . Based on the previous research conducted on the GPC mixtures incorporated nS, the range of SS was found in between 40.8 and 187.5 kg/m³, with an average

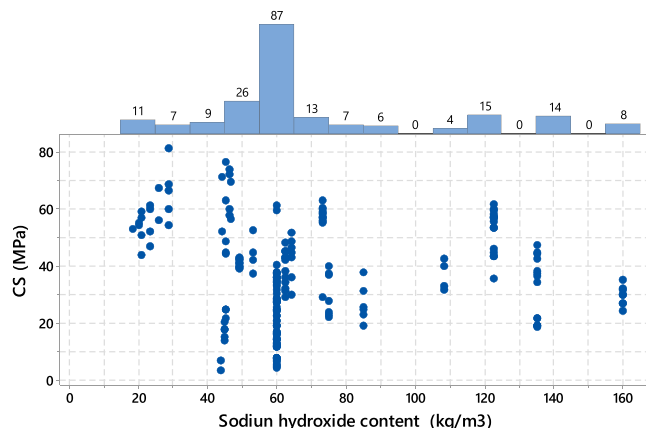


Fig. 12. Marginal plot between CS and SH content of GPC mixtures incorporated nS.

of 134.4 kg/m^3 and the standard deviations of 35.6 kg/m^3 . In comparison, other stats information like variance, skewness, and kurtosis were 1268, -1.42 , 1.55, correspondingly. Furthermore, the correlations between the CS and the SS contents of GPC can be found in Fig. 13.

5.1.7. Molarity (M)

In GPC science, the concentrations of sodium hydroxide inside water were called molarity. The authors of this study found that the molarity of SH in the collected papers was in the range between 4 and 16 M, with an average of 11.9 M and standard deviations of 3.3 M. Also, it was found that the variance of the reviewed datasets was 11.1, the skewness was -1.4 , and kurtosis was 1.3. The variations between the CS and M with the frequency of their datasets of GPC incorporated nS are presented in Fig. 14.

5.1.8. $\text{Na}_2\text{SiO}_3/\text{NaOH}$ (SS/SH)

This parameter consists of a mixture of SS and SH with the required molarity. Usually, it is prepared about 24 hrs before mixing the GPC ingredients. According to the gathered datasets, this parameter was used between 0.33 and 3, with an average of 2.05 and standard deviations of 0.76. Also, the other statistical criteria were found to be 0.59, -1.2 , and 0.22 for the variance, skewness, and kurtosis, respectively. Moreover, correlations between the CS and the SS/SH are illustrated in Fig. 15, with the frequencies of their datasets.

5.1.9. Nano-silica content (nS)

As mentioned earlier, nS was the most frequently NPs that scholars used to improve various properties of GPC composites. It was used as a binder replacement or just by the addition. Regarding the values of this input model parameter, it was found that the range of nS was used to improve GPC composites in the range between 0 and 60 kg/m^3 , with an average of 11.6 kg/m^3 , and the standard deviations of 14.5 kg/m^3 . Similarly, other statistical criteria with the correlations between the CS and the nS content can be found in Fig. 16.

5.1.10. Curing temperatures (T)

Ambient, steam, and oven curing regimes were commonly used to cure GPC composites. One of the reasons behind using NPs in GPC composites is to take away from the oven and steam curing methods and go toward ambient curing methods. Based on the collected datasets, GPC specimens modified with nS were cured in the temperature ranges between 23 and 70°C , with an average of 42.05°C and the standard deviations of 17.4°C . Also, other statistical assessment tools like variance, skewness, and kurtosis were 303.9, 0.11, and -1.92 , respectively. The variations of the CS with the nS content and the frequencies of nS datasets are presented in Fig. 17.

5.1.11. Age of specimens (A)

To gain sufficient early and late CS, the curing ages should be extended to promote the polymerization process, which strengthens geopolymers. Thus, based on the collected datasets, the cure time for GPC incorporated nS ranged from 0.5 to 180 days, with an average of 28 days and standard deviations of 31.8 days. Similarly, the published datasets' variance, skewness, and kurtosis were 1012.8, 2.36, and 6.96, respectively. The relationships between the CS and the specimen ages with the frequencies of collected data are shown in Fig. 18.

5.1.12. Compressive strength (CS)

An applied vertical load per unit area of the GPC specimens was known as normal stress or compressive strength. This property is one of the critical mechanical properties of GPC composites. As shown in Table 2, the range of the CS for the gathered datasets was in

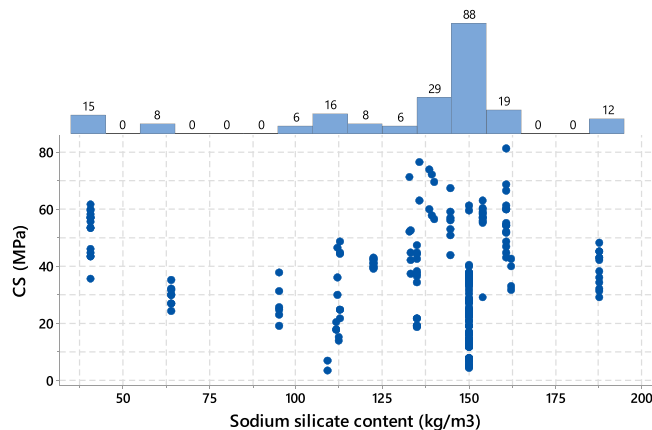


Fig. 13. Marginal plot between CS and SS content of GPC mixtures incorporated nS.

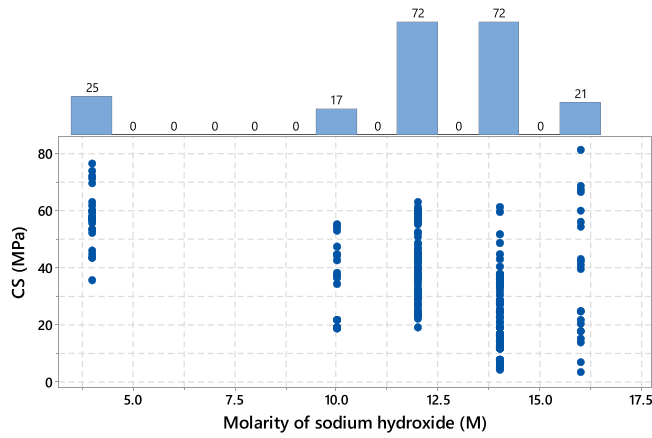


Fig. 14. Marginal plot between CS and molarity of SH of GPC mixtures incorporated nS.

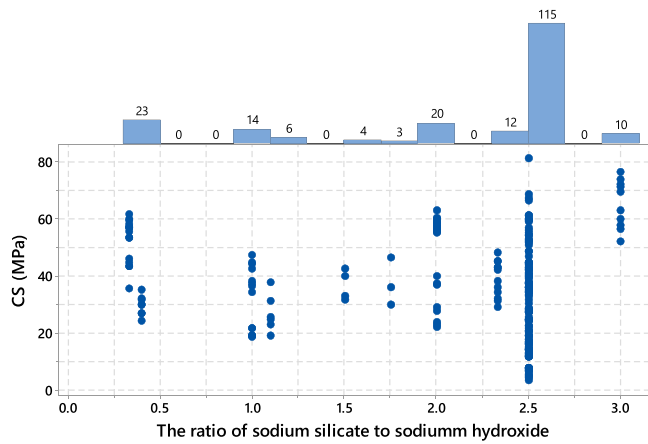


Fig. 15. Marginal plot between CS and SS/SH ratio of GPC mixtures incorporated nS.

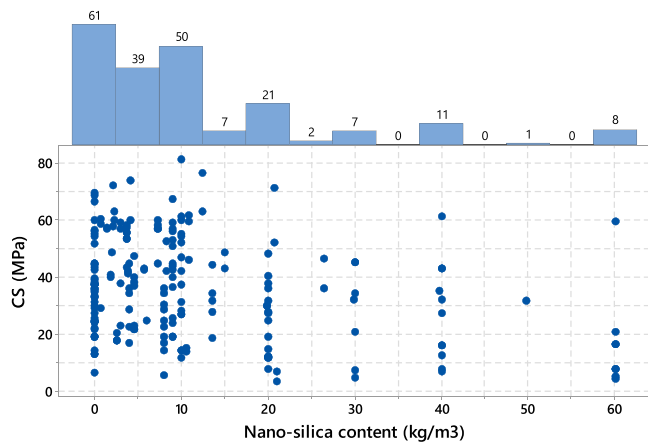


Fig. 16. Marginal plot between CS and nS content of GPC mixtures incorporated nS.

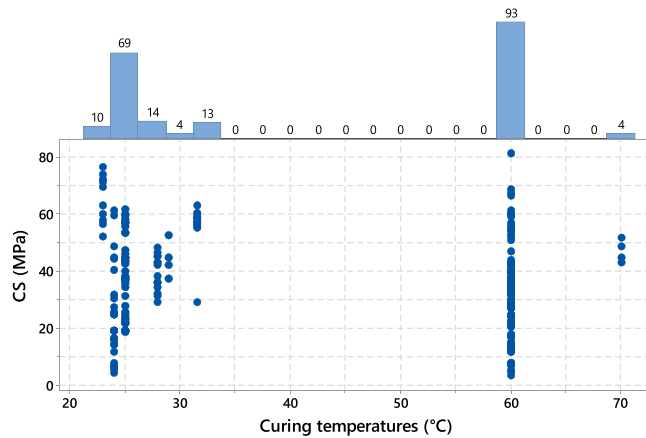


Fig. 17. Marginal plot between CS and T of GPC mixtures incorporated nS.

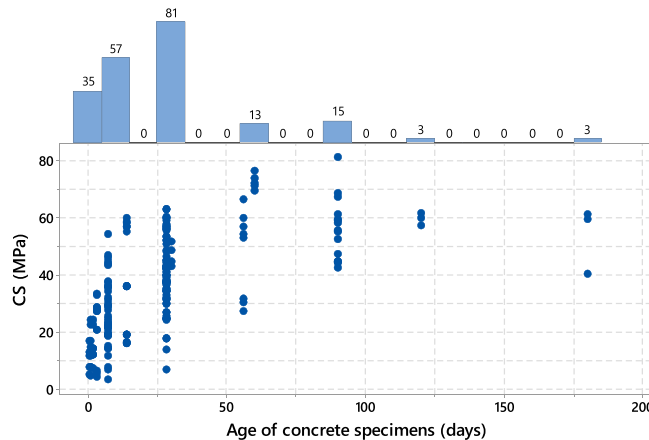


Fig. 18. Marginal plot between CS and A of GPC mixtures incorporated nS.

the range between 3.2 o 81.3 MPa, with an average of 36.2 MPa and standard deviations of 17.52 MPa. At the same time, other statistical criteria like variance, skewness, and kurtosis were 307, 0.15, and – 0.75, respectively. The histogram of the compressive strengths of the collected datasets can be found in Fig. 19.

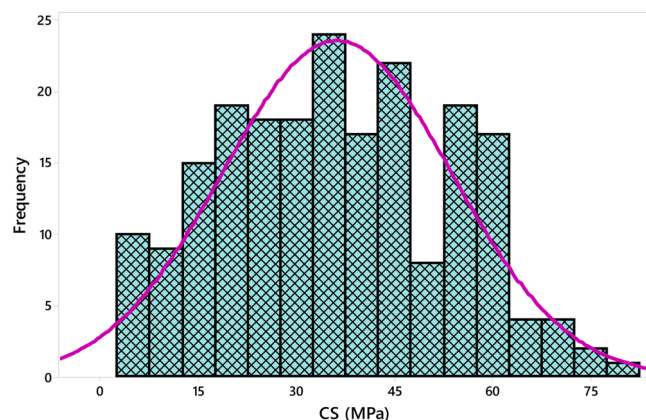


Fig. 19. The histogram of the CS of the collected datasets at different curing ages from 0.5 to 180 days.

5.2. Modeling

Based on the coefficients of the determinations (R^2) of the collected input model parameters, as shown in Figs. 8–18, there is no direct relationship between the CS and any individual input model parameters. Therefore, multiscale model techniques, including M5P, MLR, ANN, LR, and NLR, are employed to develop empirical models to forecast the CS of GPC composites incorporated nS in different mix proportion parameters curing regimes, and specimens ages.

For creating the models, the collected datasets are split into three categories. The models were built using the larger group, which included 135 datasets. The second group is made up of 36 datasets that were utilized to test the created models, and the final group is made up of 36 datasets that were consumed to validate the suggested models [29,32]. The forecasts of various models were compared employing these criteria: (1) The model's validity should be established scientifically; (2) Between estimated and tested data, it should have a lower percentage of error; (3) The RMSE, OBJ, and SI values of the suggested equations should be low, while R^2 value should be high.

5.2.1. Linear regression model (LR)

LR is one of the standard methods that scholars use to estimate and forecast the CS of concrete composites [32]. This model has a general form, as depicted in Eq. (1) [33].

$$CS = a + b(x_1) \quad (1)$$

where CS , x_1 , a and b represents the compressive strength, one of the variable input parameters, and models parameters, respectively. This equation contains just one variable of input data, so to have more practical and reliable investigations, Eq. (2) is suggested, which contains a wide range of input variable data parameters that can cover all of the geopolymer concrete mixture proportions and curing conditions, as well as curing ages.

$$CS = a + b\left(\frac{l}{b}\right) + c(b) + d(FA) + e(CA) + f(SH) + g(SS) + h(M) + i\left(\frac{SS}{SH}\right) + j(nS) + k(T) + l(A) \quad (2)$$

As mentioned earlier, all these main variables in Eq. (2) were described except that the a , b , c , d , e , f , g , h , i , j , k , and l are the model parameters. Eq. (2) is a one-of-a-kind equation because it incorporates several independent variables to generate GPC-incorporated nS that may be extremely useful in the construction industry. On the other hand, because all variables can be adjusted linearly, the proposed Eq. (2) can be considered an extension of Eq. (1).

5.2.2. Nonlinear regression model (NLR)

In terms of the NLR, Eq. (3) may be regarded as a general form for proposing an NLR model [56]. The interrelationships between the variables in Eqs. (1) and (2) can be used to calculate the CS of normal geopolymer concrete mixtures and geopolymer concrete mixtures modified with nS using Eq. (3).

$$\begin{aligned} CS = & a * \left(\frac{l}{b}\right)^b * (b)^c * (FA)^d * (CA)^e * (SH)^f * (SS)^g * (M)^h * \left(\frac{SS}{SH}\right)^i * (T)^j * (A)^k + l * \left(\frac{l}{b}\right)^m * (b)^n * (FA)^o * (CA)^p * (SH)^q \\ & * (SS)^r * (M)^s * \left(\frac{SS}{SH}\right)^t * (T)^u * (A)^v * (nS)^w \end{aligned} \quad (3)$$

where: all of the variables in this equation were provided earlier, except that the a , b , c , d , e , f , g , h , i , j , k , l , m , n , o , p , q , r , s , t , u , and v are described as a model parameter.

5.2.3. Multi-logistic regression model (MLR)

As with the previous models, the collected datasets were subjected to multi-logistic regression analysis, and the general form of the MLR is shown in Eq. (4) based on the research conducted by Mohammed et al. [57] and Faraj et al. [32]. MLR is used to distinguish a nominal predictor variable from one or more independent variables.

$$CS = a47208een \text{ model predictions of compressive strength of fly ash based geopolymer concrete mixtures using training data} * \left(\frac{l}{b}\right)^b * (b)^c * (FA)^d * (CA)^e * (SH)^f * (SS)^g * (M)^h * \left(\frac{SS}{SH}\right)^i * (nS)^j * (T)^k * (A)^l \quad (4)$$

where: all of the variables in this equation were provided earlier. Moreover, in this equation, the value of nS should be greater than 0.

5.2.4. Artificial neural network (ANN)

ANN is a powerful simulation software designed for data analysis and computation that processes and analyzes data similarly to a human brain. This machine learning tool is widely used in construction engineering to forecast the future behavior of various numerical problems [58].

An ANN model is generally divided into three main layers: input, hidden, and output. Each input and output layer can be one or more layers depending on the proposed problem. On the other hand, the hidden layer is usually ranged for two or more layers.

Although the input and output layers are generally determined by the collected data and the purpose of the designed model, the hidden layer is determined by the rated weight, transfer function, and bias of each layer to other layers. A multi-layer feed-forward network is constructed using a combination of proportions, weight/bias, and several parameters as inputs, including (l/b, b, FA, CA,,), and the output ANN is compressive strength.

There is no standardized method for designing network architecture. As a result, the number of hidden layers and neurons is determined through a trial and error procedure. One of the primary goals of the network's training process is to determine the optimal number of iterations (epochs) that provide the lowest MAE, RMSE, and best R^2 -value close to one. The effect of several epochs on lowering the MAE and RMSE has been studied. To train the designed ANN, the collected data set (a total of 207 data) was divided into three parts. Approximately 70% of the collected data was used as training data to train the network. The data set was tested with 15% of the total data, and the remaining data were used to validate the trained network [59]. The designed ANN was trained and tested for various hidden layers to determine optimal network structure based on the fitness of the predicted CS of GPC incorporated nS with the CS of the actual collected data. It was observed that the ANN structure with two hidden layers, 24 neurons, and a hyperbolic tangent transfer function was a best-trained network that provides a maximum R^2 and minimum both MAE and RMSE (shown in Fig. 20). As a part of this work, an ANN model has been used to estimate the future value of the CS of GPC incorporated nS. The general equation of the ANN model is shown in Eqs. (5)–(7).

From linear node 0:

$$CS = Threshold + \left(\frac{Node_1}{1 + e^{-B1}} \right) + \left(\frac{Node_2}{1 + e^{-B2}} \right) + \dots \quad (5)$$

From sigmoid node 1:

$$B1 = Threshold + \sum (\text{Attribute} * \text{Variable}) \quad (6)$$

From sigmoid node 2:

$$B2 = Threshold + \sum (\text{Attribute} * \text{Variable}) \quad (7)$$

5.2.5. M5P-tree model (M5P)

The M5P model tree reconstructs Quinlan's M5P-tree algorithm [60], a decision tree added to the leaves nodes with a linear regression function. The decision tree encapsulates the algorithms in a tree structure formed by nodes formed during training on data. The decision tree nodes are classified as root nodes, internal nodes, and leaf nodes. Nodes are interconnected through branches until the leaves are reached [61]. Mohammed [62] also introduced the M5P-tree as a robust decision tree learner model for regression analysis. This learner algorithm places the linear regression functions at the terminal nodes. Classifying all data sets into multiple sub-spaces assigns a multivariate linear regression model to each sub-space. The M5P-tree algorithm operates on continuous class problems rather than discrete segments and can handle tasks with a high number of dimensions. It reveals the developed information of each linear model component constructed to estimate the nonlinear correlation of the data sets. The information about division criteria for the M5-tree model is obtained through the error calculation at each node. The standard deviation of the class entering that node at each node is used to analyze errors. At each node, the attribute that maximizes the reduction of estimated error is used to evaluate any task performed by that node. As a result of this division in the M5P tree, a large tree-like structure will be generated, which will result in

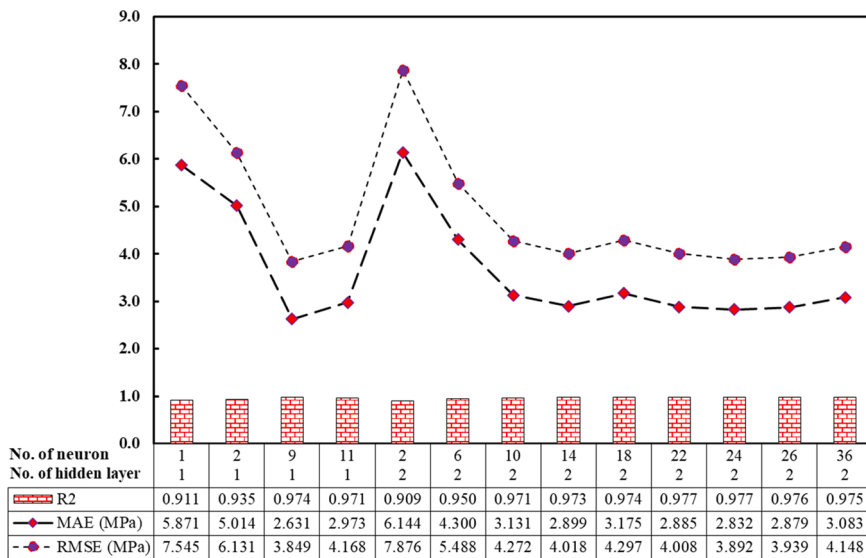


Fig. 20. Choosing best-hidden layer and neurons for ANN model based on R^2 , MAE, and RMSE values.

overfitting. The enormous tree is trimmed in the followed step, and linear regression functions restore the pruned subtrees. The general equation form of the M5P-tree model is the same as the linear regression equation, as shown in Eq. (8).

$$CS = a + b \left(\frac{l}{b} \right) + c(b) + d(FA) + e(CA) + f(SH) + g(SS) + h(M) + i \left(\frac{SS}{SH} \right) + j(nS) + k(T) + l(A) \quad (8)$$

where: the descriptions of all of the variables in this Eq. (8) were provided earlier.

5.3. Model efficiencies

To rate and assess the proposed models' accuracy, various performance stats tools such as R^2 , RMSE, MAE, SI, and OBJ were used, which they have the following equations:

$$R^2 = \left(\frac{\sum_{p=1}^p (y_p - \bar{y})(x_p - \bar{x}')}{\sqrt{\left[\sum_{p=1}^p (y_p - \bar{y}')^2 \right] \left[\sum_{p=1}^p (x_p - \bar{x}')^2 \right]}} \right)^2 \quad (9)$$

$$RMSE = \sqrt{\frac{\sum_{p=1}^p (x_p - y_p)^2}{n}} \quad (10)$$

$$MAE = \frac{\sum_{p=1}^p |(x_p - y_p)|}{n} \quad (11)$$

$$SI = \frac{RMSE}{\bar{y}'} \quad (12)$$

$$OBJ = \left(\frac{n_{tr}}{n_{all}} * \frac{RMSE_{tr} + MAE_{tr}}{R_{tr}^2 + 1} \right) + \left(\frac{n_{tst}}{n_{all}} * \frac{RMSE_{tst} + MAE_{tst}}{R_{tst}^2 + 1} \right) + \left(\frac{n_{val}}{n_{all}} * \frac{RMSE_{val} + MAE_{val}}{R_{val}^2 + 1} \right) \quad (13)$$

where:

x_p and y_p are estimated and tested CS values, \bar{y}' and \bar{x}' are averages of experimentally tested and the estimated values from the models, respectively. **tr**, **tst**, and **val** are referred to the training, testing, and validating datasets, respectively, and **n** is the number of datasets. Except for the R^2 value, zero is the optimal value for all other evaluation parameters. However, one is the highest benefit for R^2 . Regarding the SI parameter, it can be said that a model has a (poor performance) when $SI > 0.3$, a (fair performance) when $0.2 < SI < 0.3$, a (good performance) when $0.1 < SI < 0.2$, and an (excellent performance) when $SI < 0.1$ [32]. Furthermore, the OBJ parameter was employed as a performance measurement parameter in Eq. (13) to measure the efficiency of the suggested models.

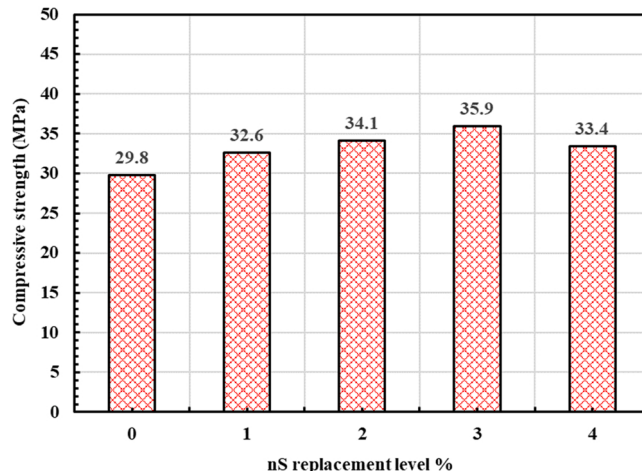


Fig. 21. Compressive strength of geopolymer concrete at various nS dosages at 28 days (current study).

6. Results and analysis

6.1. Experimental

The influences of adding nano-silica on the compressive strength of GGBFS-based geopolymer concrete is illustrated in Fig. 21. This test has been carried out on a 100 * 200 mm cylinder based on ASTM C39. It was found that the compressive strength was improved as the dosage on nano-silica increased up to 3%, and then it was decreased. For instance, the compressive strength was improved by 9.4%, 14.43%, and 20.47% at 1%, 2%, and 3% of nS dosages, respectively, compared to the control GPC mixture without any dosages of nS. This result was attributed to filling nanopores inside the geopolymer concrete with silica nanoparticles that make the matrix denser and more compact. In addition, the chemical composition of the nS, which is rich in silica, accelerates the geopolymer reactions and makes the geopolymer binder stronger, which eventually enhances the strength of the specimens [21]. On the other hand, the compressive enhancement was decreased by 7% at 4% of nS dosage, compared to the optimum (3%) dosages of the nS content. This reduction in the compressive strength was attributed to the overflowing availability of unreacted nS particles in the matrix. The excess amount of nS causes agglomerations between the nS particles that could have prohibited the silica dissolution, thereby leading to producing of voids. Also, poor dispersion of nS inside geopolymer concrete mixture negatively affects the performance of GPC mixtures, as a consequence decreasing the compressive strength of the geopolymer concrete [22,63].

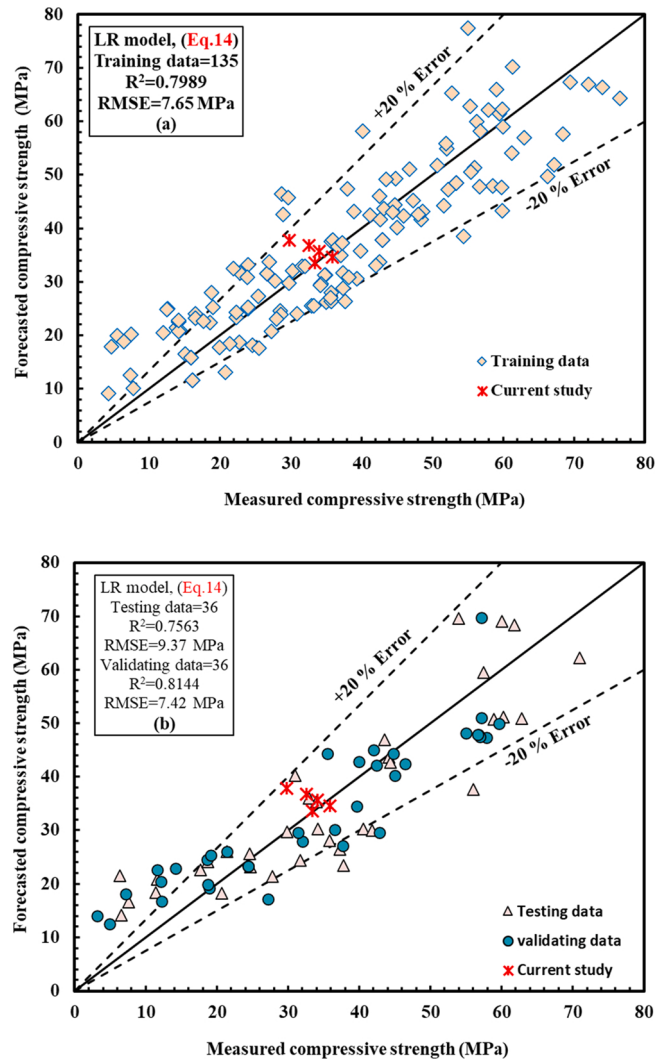


Fig. 22. Comparison between tested and predicted CS of GPC mixtures incorporated nS using LR model, (a) training data with current study results, (b) testing and validating data with current study results.

6.2. Modeling

6.2.1. LR model

The output of this model revealed that the l/b , SS/SH, and M are those parameters that have a greater impact on the CS of GPC incorporated nS than other parameters. This result was confirmed by a wide range of published experimental works in the literature [64–66]. Eq. (14) with the weight of each model parameter is the output of this model. Optimizing the sum of error squares and the least square method, which were implemented in an Excel program using Solver to calculate the ideal value for the equation in one cell designated the objective cell, were used to determine the weighting of each parameter on the CS of GPC mixtures incorporating nS. The values of other equation cells constrained this object cell in the worksheet [32,57].

$$CS = 110.06 - 66.6 \left(\frac{l}{b} \right) + 0.06(b) - 0.01(FA) + 0.005(CA) - 0.34(SH) + 0.12(SS) - 3.12(M) - 13.9 \left(\frac{SS}{SH} \right) - 0.18(nS) + 0.11(T) + 0.23(A) \quad (14)$$

Fig. 22a and b depict the relationship between estimated and real CS of GPC mixtures incorporated nS for training, testing, validating, and current experimental datasets. Moreover, this model was evaluated by some statistical assessment tools, and it was observed that the R^2 and RMSE for the training datasets were equal to 0.7989 7.65 MPa, respectively. As illustrated in Figs. 23 and 24, the other statistical criteria like OBJ and SI were 8.05 MPa and 0.209. Finally, utilizing the training, testing, validating, and current study datasets normalized forecasted CS/ measured CS versus the number of datasets for all the models were evaluated, as shown in Fig. 25.

6.2.2. NLR model

The correlations between the actual and forecasted CS of GPC mixtures incorporated nS are presented in Fig. 26a and b for the training, testing, validating, current study datasets. As shown in Eq. (15), the weight of the model parameters demonstrated that the l/b , SH, and M are those input variable parameters that significantly affect the CS of geopolymer concrete mixtures modified with nS. This result was also well-validated in the previous experimental laboratory research works [64,67,68].

$$CS = -4643005 * \left(\frac{l}{b} \right)^{3.78} * (b)^{1.34} * (FA)^{-1.87} * (CA)^{0.08} * (SH)^{5.5} * (SS)^{-7.85} * (M)^{2.72} * \left(\frac{SS}{SH} \right)^{-6.06} * (T)^{-0.53} * (A)^{0.02} + 73.89 \\ * \left(\frac{l}{b} \right)^{0.37} * (b)^{-0.03} * (FA)^{-0.45} * (CA)^{0.44} * (SH)^{-0.15} * (SS)^{-0.001} * (M)^{-0.02} * \left(\frac{SS}{SH} \right)^{-0.15} * (T)^{0.0002} * (A)^{0.15} * (nS)^{0.002} \quad (15)$$

Similar to the LR model, this model was also assessed by some statistical criteria, and it was found that the R^2 , RMSE, OBJ, and SI of the training datasets were equal to 0.8792, 5.92 MPa 5.80 MPa, and 0.162, respectively.

6.2.3. MLR model

Eq. (16) shows the generated models for the MLR model with various variable parameters. The most significant independent factors that impact the CS of the geopolymer concrete mixtures modified with nS in the MLR model were SS content, age of the specimens, and curing temperatures, which are matched with some experimental studies published in the past articles [68,69].

$$CS = 29.0347208 \text{een model predictions of compressive strength of fly ash based geopolymer concrete mixtures} \\ \text{using training data} * \left(\frac{l}{b} \right)^{-1.47} * (b)^{0.04} * (FA)^{-0.21} * (CA)^{-0.26} * (SH)^{-0.09} * (SS)^{0.56} * (M)^{-0.49} * \left(\frac{SS}{SH} \right)^{-0.22} * (nS)^{-0.005} \\ * (T)^{0.13} * (A)^{0.2} \quad (16)$$

Fig. 27a was created by utilizing training datasets to depict the anticipated and measured CS correlations for the GPC mixtures incorporated nS. Furthermore, similar to the earlier models, this model was tested using two parts of data (validating and testing data) to demonstrate its efficacy for variables not included in the model data (training data). The findings indicate that by substituting the independent variables into the established equation, this model can predict the CS of GPC, as illustrated in Fig. 27b. the value of R^2 RMSE for this developed model are 0.7787 8.02 MPa, respectively, for the training datasets. Also, as depicted in Figs. 23 and 24, other statistical assessment tools like OBJ and SI values were observed at 8.8 MPa and 0.22, respectively.

6.2.4. ANN model

In this study, the authors tried a lot to get the high efficiency of the ANN by applying different numbers of the hidden layer, neurons, momentum, learning rate, and iteration, as can be seen in Fig. 20. Lastly, it was observed that when the ANN has two hidden layers, 24 neurons (12 for left side and 12 for the right side as shown in Fig. 28), 0.2 momenta, 0.1 learning rate, and 2000 iterations give best-predicted values of the CS of the GPC mixtures incorporated nS. The ANN model was equipped with the training datasets, accompanied by testing and validating datasets to predict the compression strength values for the correct input parameters. The comparison between estimated and experimentally tested CS of GPC mixtures incorporated nS for training, testing, validating, and current study datasets are presented in Fig. 29a and b. The consumed data have a + 10% and – 20% error line for the training and testing datasets, and ± 10% for the validating datasets, which is better than the other developed models. Furthermore, this model has a better performance

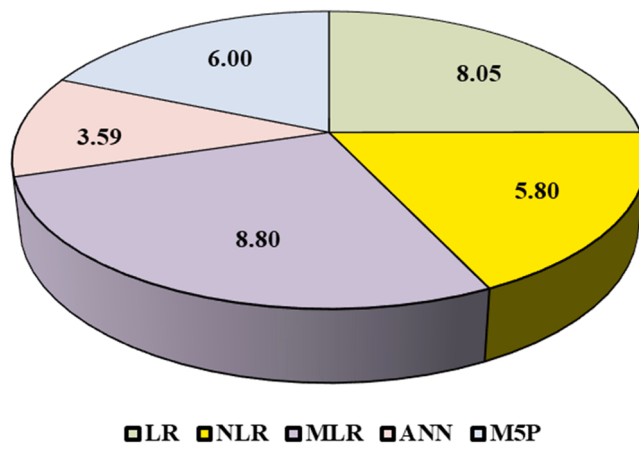


Fig. 23. The OBJ values of all developed models.

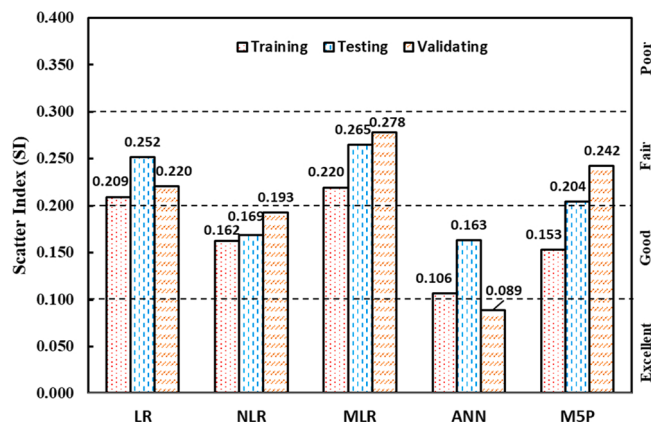


Fig. 24. Comparing the SI performance parameter of different developed models.

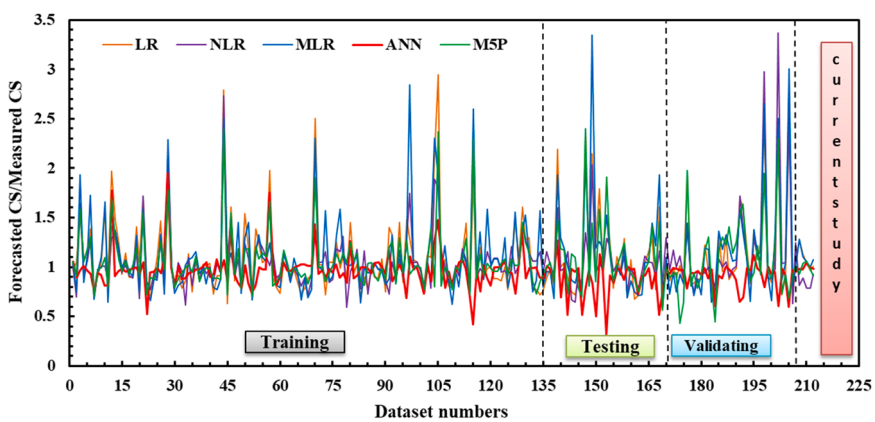


Fig. 25. Residual error diagram of CS of GPC mixtures incorporated nS using the whole datasets for all models.

than other models to predict the CS of the GPC incorporated nS based on the value of OBJ and SI illustrated in Figs. 23 and 24. Also, the value of $R^2 = 0.9771$, MAE = 2.83 MPa, and RMSE = 3.89 MPa. Finally, utilizing the training, testing, validating, and current study datasets normalized forecasted CS/ measured CS versus the number of datasets for all the models were evaluated, as shown in Fig. 25.

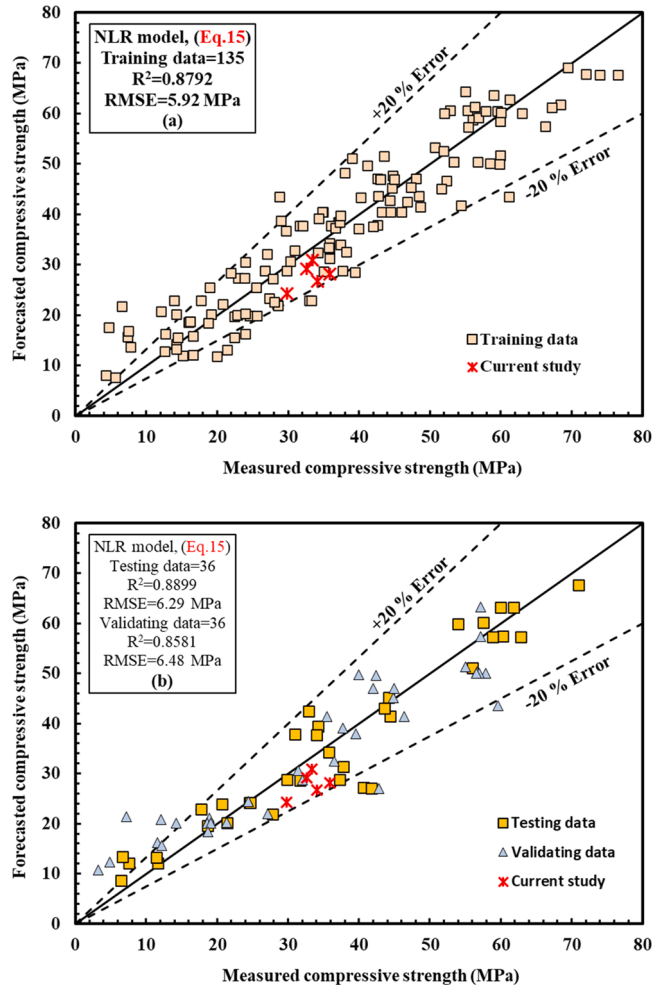


Fig. 26. Comparison between tested and predicted CS of GPC mixtures incorporated nS using NLR model, (a) training data with current study results, (b) testing and validating data with current study results.

6.2.5. M5P-tree model

The predicted and observed CS of the GPC mixtures incorporated nS for whole the datasets are shown in Fig. 30a and b. Similar to the other models, it was discovered that the l/b and M of the GPC mixtures incorporated nS has the greatest impact on the CS of the GPC mixtures incorporated nS, which agrees with experimental findings in the past studies [64,67,68]. Fig. 31 shows the tree-shaped branch correlations. Also, the model (in Eq. (17)) parameters are summarized in Table 5, and the model variables will be selected based on the linear tree registration function.

$$CS = a + b \left(\frac{l}{b} \right) + c(b) + d(FA) + e(CA) + f(SH) + g(SS) + h(M) + i \left(\frac{SS}{SH} \right) + j(nS) + k(T) + l(A) \quad (17)$$

For all of the training, testing, and validation datasets, there is a 20% error line. Furthermore, this model's R^2 , RMSE, MAE, OBJ, and SI evaluation criteria are 0.9454, 5.59 MPa, 4.45 MPa, 6.0 MPa, and 0.153, respectively, for the training datasets.

6.3. Experimental results and proposed models

The developed models were evaluated and tested by using current experimental laboratory results. All input model parameters were employed to get the predicted compressive strength of current geopolymer concrete specimens. As shown in Figs. 22, 26, 27, 29, and 30) and Table 6, the developed models could be used to predict the compressive strength of current experimental results. For example, the experimental compressive strength results at 0%, 1%, 2%, 3%, and 4% dosages of nS was 29.8, 32.6, 34.1, 35.9, and 33.4 MPa, respectively; on the other hand, when the model parameter of these mixtures were employed in LR model, the predicted compressive strength became 37.8, 36.74, 35.68, 34.61, and 33.55 MPa. This result revealed that this model overestimate the compressive strength of current GPC mixtures by 8, 4.14, 1.58, and 0.15 MPa for dosages of nS 0%, 1%, 2%, and 4%, correspondingly,

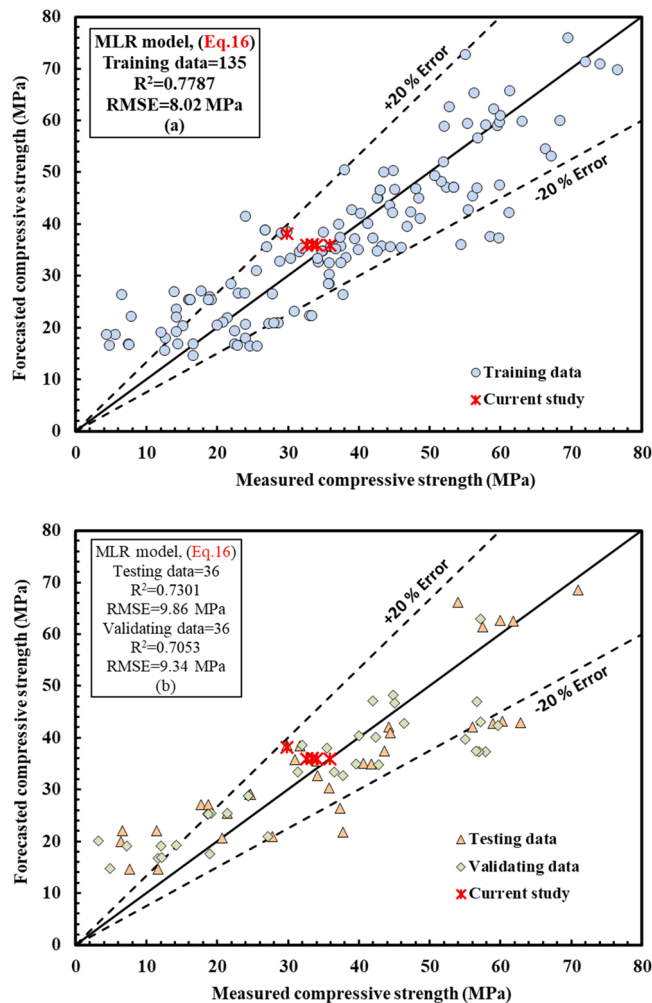


Fig. 27. Comparison between tested and predicted CS of GPC mixtures incorporated nS using MLR model, (a) training data with current study results, (b) testing and validating data with current study results.

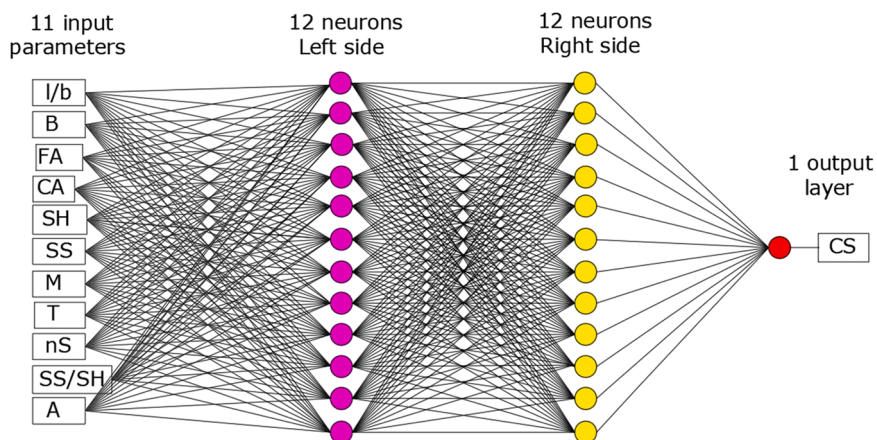


Fig. 28. Optimal network structures of the ANN model.

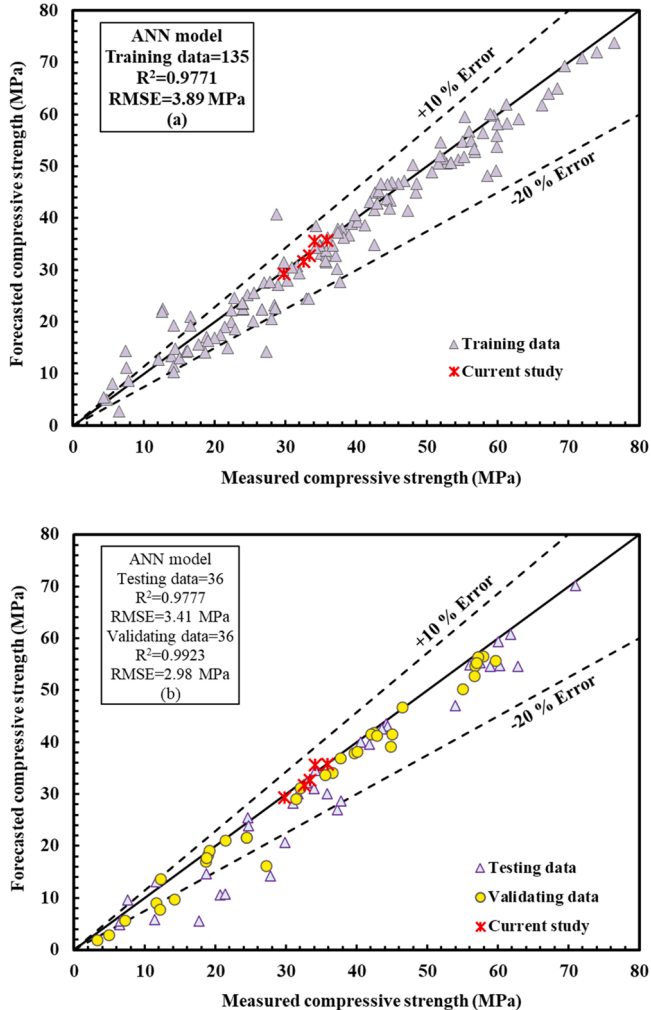


Fig. 29. Comparison between tested and predicted CS of GPC mixtures incorporated nS using ANN model, (a) training data with current study results, (b) testing and validating data with current study results.

and underestimate the compressive strength by 1.29 MPa, at 3% nS percent. However, the difference between experimental and predicted compressive strength of geopolymer concrete mixtures incorporated previous dosages of nS were 0.5, 0.9, -1.5, 0.2, and 0.7 MPa, respectively, for the ANN model, and 5.5, 3.5, 7.4, 7.77, and 2.58 MPa, for NLR model. Finally, it can be concluded that these models could be used for preliminary forecasting of the compressive strength of geopolymer concrete composites incorporated different dosages of nano-silica.

6.4. Proposed models performance

As early mentioned, the efficiency of the developed models was evaluated by employing these five stats tools: RMSE, MAE, SI, OBJ, and R^2 . Compared to the LR, NLR, MLR, and M5P models, the ANN model has a higher R^2 with lower RMSE and MAE values and lower OBJ and SI values.

In addition, Fig. 32 shows a comparison of model predictions of the CS of GPC mixtures incorporated nS based on the testing datasets. Furthermore, Fig. 25 displays the normalized forecasted CS/ measured CS versus the number of datasets for all the models. The whole figures show that the estimated and tested CS values for the ANN model are close, indicating that the ANN model is more accurate than other models.

Fig. 23 shows the OBJ values for all of the proposed models. The OBJ is 8.05, 5.8, 8.8, 3.59, and 6.0 for LR, NLR, MLR, ANN, and M5P, respectively. The ANN model has a lower OBJ value, about 124% less than the LR model, 61.5% less than the NLR model, 145% less than the MLR model, and 67% less than the M5P model. This also emphasized that the ANN model better forecasts the CS of GPC incorporated nS.

In addition, Fig. 24 shows the SI values for the created models during the training, validating, and testing phases. The SI values for

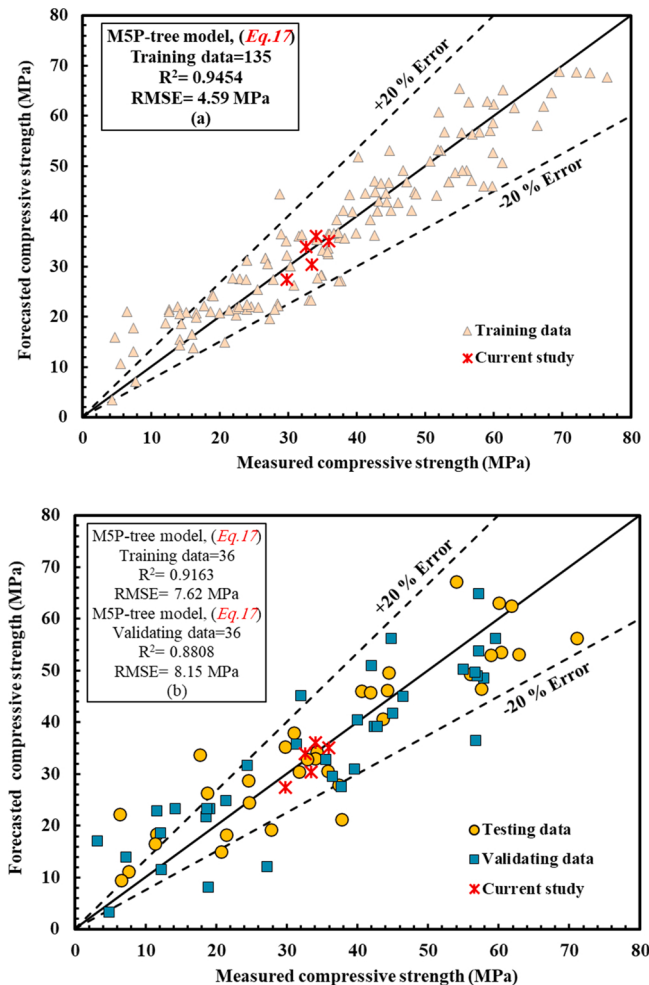


Fig. 30. Comparison between tested and predicted CS of GPC mixtures incorporated nS using M5P-tree model, (a) training data with current study results, (b) testing and validating data with current study results.

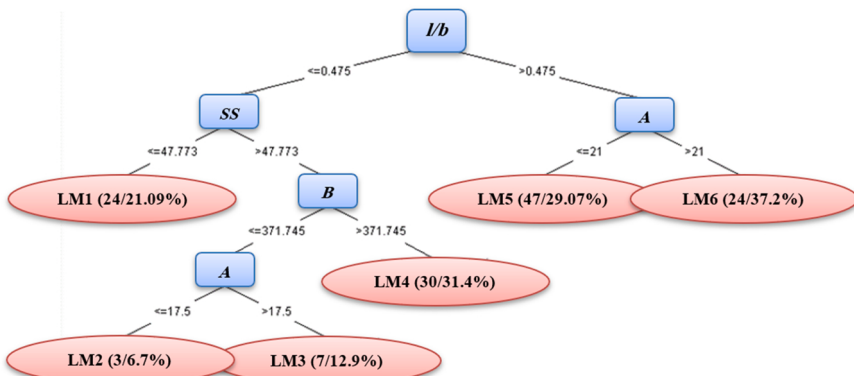


Fig. 31. M5P-tree Pruned model tree.

NLR and ANN models for the entire training, testing, and validating datasets were between 0.1 and 0.2, signalizing good accuracy for these models. While, for the other remaining models, the values of SI were between 0.2 and 0.3, this result revealed that the performance of the LR, MLR and M5P models is in fair condition. Similar to other statistical assessment criteria, the ANN model has smaller SI values among the entire model. The ANN model has lower SI values (for training datasets) than the LR, NLR, MLR, and M5P

Table 5

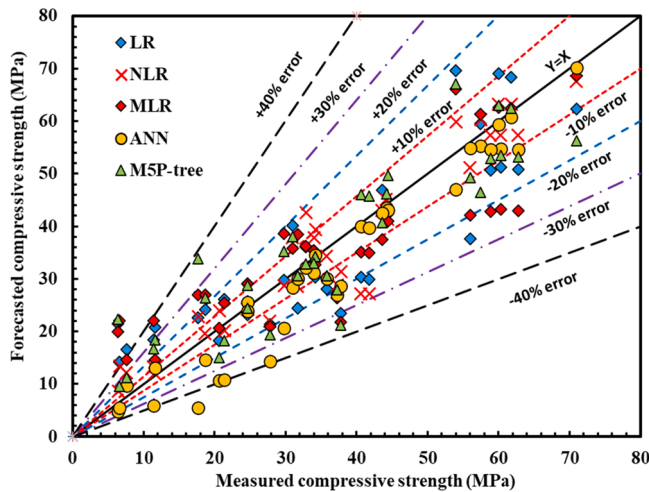
M5P-tree model parameters (Eq. (17)).

(LM) num:	1	2	3	4	5	6
<i>a</i>	- 93.696	+32.7126	+32.8862	- 2.7578	- 166.0773	- 13.196
<i>b</i>	274.4776	38.4951	38.4951	38.4951	141.2642	53.0334
<i>c</i>	+0.0488	- 0.0138	- 0.0138	+0.0534	+0.1562	+0.0806
<i>d</i>					+0.0655	+0.024
<i>e</i>	+0.0029	+0.0077	+0.0077	+0.0174		- 0.0269
<i>f</i>	+0.2796	- 0.0513	- 0.0513	- 0.1534	- 0.0386	- 0.0386
<i>g</i>	- 0.0501	+0.0119	+0.0119	- 0.0114	- 0.0154	- 0.0154
<i>h</i>	- 0.5772	- 0.8632	- 0.8632	- 0.8632	- 0.4692	- 0.4692
<i>i</i>						
<i>j</i>	- 0.0307	- 0.0307	+0.0683	+0.0516	- 0.0282	- 0.0282
<i>k</i>					+0.3218	+0.077
<i>l</i>	+0.1921	+0.1625	+0.1575	+0.2233	+0.9407	+0.181

Table 6

Comparison between current experimental CS results and predicted CS of proposed models.

Experimental Results (ER)	29.8	32.6	34.1	35.9	33.4
Predicted-LR	37.80	36.74	35.68	34.61	33.55
ER-LR	-8.00	-4.14	-1.58	1.29	-0.15
Predicted-NLR	24.3	29.1	26.7	28.13	30.82
ER-NLR	5.5	3.5	7.4	7.77	2.58
Predicted-MLR	38.14	35.94	35.91	35.95	36.01
ER-MLR	-8.34	-3.34	-1.81	-0.05	-2.61
Predicted-ANN	29.3	31.7	35.6	35.7	32.7
ER-ANN	0.5	0.9	-1.5	0.2	0.7
Predicted-M5P	27.5	33.9	36.1	35.1	30.4
ER-M5P	2.3	-1.3	-2	0.8	3

**Fig. 32.** Comparison between model predictions of CS of GPC mixtures incorporated nS using testing datasets.

models by 97.2%, 52.8%, 107.5%, and 44.3%, respectively. This also demonstrated that when forecasting the CS of GPC mixtures incorporated nS, the ANN model is more efficient and performs better than the other models.

7. Conclusions

Based on the results of this study, the following conclusions are drawn:

1. NPs used in GPC mixtures include nano-silica, nano-clay, nano-alumina, carbon nanotubes, nano-titanium, and nano-metakaolin. The most common of these was nano-silica.
2. Most of the time, all types of NPs were used as binder replacements in the production of different geopolymers composites, with small percentage substitutions mostly less than 5%.

3. The average percentage of nS used in GPC mixtures was approximately 3% of the binder content.
4. In the GPC, NPs do three things: They fill in the pores and voids, speed up chemical reactions between the ingredients in GPC mixtures, and improve the transition zones between them.
5. Based on the current experimental results, 3% of nS dosage was the optimum content for getting the maximum compressive strength of GPC.
6. The LR, NLR, MLR, ANN, and M5P-tree models have been used successfully to develop predictive models for the CS of nS-containing GPC mixtures. The estimated CS of GPC mixtures containing nS was close to the experimentally determined CS.
7. According to statistical evaluation and sensitivity analysis, the ANN model outperforms the other four models. R^2 values are 0.9771, 0.9777, and 0.9923 for training, testing, and validating datasets. The training dataset's RMSE, MAE, OBJ, and SI statistics are 3.892 MPa, 2.832 MPa, 3.59 MPa, and 0.106, respectively.
8. The obtained results indicate that the most significant variable parameters for estimating the CS of GPC mixtures contained nS are the l/b, SS/SH, M, T, and A.

Declaration of Competing Interest

The authors declare that they have no known competing financial interests or personal relationships that could have appeared to influence the work reported in this paper.

References

- [1] N. Hamah Sor, N. Hilal, R.H. Faraj, H.U. Ahmed, A.F.H. Sherwani, Experimental and empirical evaluation of strength for sustainable lightweight self-compacting concrete by recycling high volume of industrial waste materials, *Eur. J. Environ. Civ. Eng.* (2021) 1–18, <https://doi.org/10.1080/19648189.2021.1997827>.
- [2] R.H. Faraj, H.U. Ahmed, A.F.H. Sherwani, Fresh and mechanical properties of concrete made with recycled plastic aggregates. *Handbook of Sustainable Concrete and Industrial Waste Management*, Woodhead Publishing, 2022, pp. 167–185, <https://doi.org/10.1016/B978-0-12-821730-6.00023-1>.
- [3] M.A. Khan, S.A. Memon, F. Farooq, M.F. Javed, F. Aslam, R. Alyousef, Compressive strength of fly-ash-based geopolymers concrete by gene expression programming and random forest, *Adv. Civ. Eng.* (2021) 2021, <https://doi.org/10.1155/2021/6618407>.
- [4] N. Mahasenan, S. Smith, K. Humphreys, The cement industry and global climate change: current and potential future cement industry CO₂ emissions, in: *Proceedings of the Greenhouse Gas Control Technologies-6th International Conference*, Pergamon, 2003, pp. 995–1000.
- [5] F.U.A. Shaikh, Mechanical and durability properties of fly ash geopolymers concrete containing recycled coarse aggregates, *Int. J. Sustain. Built Environ.* 5 (2) (2016) 277–287, <https://doi.org/10.1016/j.ijsb.2016.05.009>.
- [6] G. Yildirim, M. Sahmaran, H.U. Ahmed, Influence of hydrated lime addition on the self-healing capability of high-volume fly ash incorporated cementitious composites, *J. Mater. Civ. Eng.* 27 (6) (2015) 04014187, [https://doi.org/10.1061/\(ASCE\)MT.1943-5533.0001145](https://doi.org/10.1061/(ASCE)MT.1943-5533.0001145).
- [7] J.L. Provis, A. Palomo, C. Shi, Advances in understanding alkali-activated materials, *Cem. Concr. Res.* 78 (2015) 110–125, <https://doi.org/10.1016/j.cemconres.2015.04.013>.
- [8] H.A. Abdel-Gawad, S.A. Abo-El-Enein, A novel method to produce dry geopolymers cement powder, *HBRC J.* 12 (1) (2016) 13–24, <https://doi.org/10.1016/j.hbrcj.2014.06.008>.
- [9] M. Weil, K. Dombrowski, A. Buchwald, Life-cycle analysis of geopolymers. *Geopolymers*, Woodhead Publishing, 2009, pp. 194–210, <https://doi.org/10.1533/9781845696382.2.194>.
- [10] J. Davidovits, *Geopolymer Chemistry and Applications*, 4th ed., J. Davidovits.–Saint-Quentin, France, 2015.
- [11] S.M. Qaidi, B.A. Tayeh, A.M. Zeyad, A.R. de Azevedo, H.U. Ahmed, W. Emad, Recycling of mine tailings for the geopolymers production: a systematic review, *Case Stud. Constr. Mater.* (2022), e00933, <https://doi.org/10.1016/j.cscm.2022.e00933>.
- [12] H.U. Ahmed, A.A. Mohammed, S. Rafiq, A.S. Mohammed, A. Mosavi, N.H. Sor, S. Qaidi, Compressive strength of sustainable geopolymers concrete composites: a state-of-the-art review, *Sustainability* 13 (24) (2021) 13502, <https://doi.org/10.3390/su132413502>.
- [13] M.T. Marvila, A.R.G.D. Azevedo, C.M.F. Vieira, Reaction mechanisms of alkali-activated materials, *Rev. IBRACON Estrut. Mater.* (2021) 14, <https://doi.org/10.1590/S1983-41952021000300009>.
- [14] S.M. Qaidi, B.A. Tayeh, H.F. Isleem, A.R. de Azevedo, H.U. Ahmed, W. Emad, Sustainable utilization of red mud waste (bauxite residue) and slag for the production of geopolymers composites: a review, *Case Stud. Constr. Mater.* (2022), e00994, <https://doi.org/10.1016/j.cscm.2022.e00994>.
- [15] B.C. Mendes, L.G. Pedrotti, C.M.F. Vieira, M. Marvila, A.R. Azevedo, J.M.F. de Carvalho, J.C.L. Ribeiro, Application of eco-friendly alternative activators in alkali-activated materials: a review, *J. Build. Eng.* 35 (2021), 102010, <https://doi.org/10.1016/j.jobe.2020.102010>.
- [16] A.R. de Azevedo, M.T. Marvila, H.A. Rocha, L.R. Cruz, C.M.F. Vieira, Use of glass polishing waste in the development of ecological ceramic roof tiles by the geopolymmerization process, *Int. J. Appl. Ceram. Technol.* 17 (6) (2020) 2649–2658, <https://doi.org/10.1111/ijac.13585>.
- [17] A.R. De Azevedo, M. Teixeira Marvila, L. Barbosa de Oliveira, W. Macario Ferreira, H. Colorado, S. Rainho Teixeira, C. Mauricio Fontes Vieira, Circular economy and durability in geopolymers ceramics pieces obtained from glass polishing waste, *Int. J. Appl. Ceram. Technol.* 18 (6) (2021) 1891–1900, <https://doi.org/10.1111/ijac.13780>.
- [18] A.A. Mohammed, H.U. Ahmed, A. Mosavi, Survey of mechanical properties of geopolymers concrete: a comprehensive review and data analysis, *Materials* 14 (16) (2021) 4690, <https://doi.org/10.3390/ma14164690>.
- [19] M.C. Rocío, R.S. Williams, P. Alivisatos (Eds.), *Nanotechnology Research Directions: IWGN Workshop Report: Vision for Nanotechnology in the Next Decade*, Springer Science & Business Media, 2000.
- [20] H.H. Sharif, Fresh and mechanical characteristics of eco-efficient geopolymers concrete incorporating nano-silica: an overview, *Kurd. J. Appl. Res.* (2021) 64–74, <https://doi.org/10.24017/science.2021.2.6>.
- [21] H.U. Ahmed, A.A. Mohammed, A.S. Mohammad, The role of nanomaterials in geopolymers concrete composites: A state-of-the-art review, *J. Build. Eng.* (2022), 104062, <https://doi.org/10.1016/j.jobe.2022.104062>.
- [22] S.M. Mustakim, S.K. Das, J. Mishra, A. Aftab, T.S. Alomayri, H.S. Assadi, C.R. Kaze, Improvement in fresh, mechanical and microstructural properties of fly ash-blast furnace slag based geopolymers concrete by addition of nano and micro silica, *Silicon* (2020) 1–14, <https://doi.org/10.1007/s12633-020-00593-0>.
- [23] A. Ravithea, N.K. Kumar, A study on the effect of nano clay and GGBS on the strength properties of fly ash based geopolymers, *Mater. Today Proc.* 19 (2019) 273–276, <https://doi.org/10.1016/j.mtpr.2019.06.761>.
- [24] F. Shahrajabian, K. Behfarnia, The effects of nano particles on freeze and thaw resistance of alkali-activated slag concrete, *Constr. Build. Mater.* 176 (2018) 172–178, <https://doi.org/10.1016/j.conbuildmat.2018.05.033>.
- [25] M.A. Kotop, M.S. El-Feky, Y.R. Alharbi, A.A. Abadel, A.S. Binyahya, Engineering properties of geopolymers concrete incorporating hybrid nanomaterials, *Ain Shams Eng. J.* (2021), <https://doi.org/10.1016/j.asej.2021.04.022>.
- [26] E. Rabiaa, R.A.S. Mohamed, W.H. Sofi, T.A. Tawfik, Developing geopolymers concrete properties by using nanomaterials and steel fibers, *Adv. Mater. Sci. Eng.* (2020) 2020, <https://doi.org/10.1155/2020/5186091>.

- [27] K.G.K. Sastry, P. Sahitya, A. Ravitheja, Influence of nano TiO₂ on strength and durability properties of geopolymers concrete, *Mater. Today Proc.* 45 (2021) 1017–1025, <https://doi.org/10.1016/j.matpr.2020.03.139>.
- [28] H.U. Ahmed, R.H. Faraj, N. Hilal, A.A. Mohammed, A.F.H. Sherwani, Use of recycled fibers in concrete composites: a systematic comprehensive review, *Compos. Part B Eng.* (2021), 108769, <https://doi.org/10.1016/j.compositesb.2021.108769>.
- [29] E.M. Golafshani, A. Behnood, M. Arashpour, Predicting the compressive strength of normal and high-performance concretes using ANN and ANFIS hybridized with Grey Wolf Optimizer, *Constr. Build. Mater.* 232 (2020), 117266, <https://doi.org/10.1016/j.conbuildmat.2019.117266>.
- [30] A.A. Shahmansouri, H.A. Bengar, S. Ghanbari, Compressive strength prediction of eco-efficient GGBS-based geopolymers concrete using GEP method, *J. Build. Eng.* (2020), 101326, <https://doi.org/10.1016/j.jobe.2020.101326>.
- [31] M. Velay-Lizancos, J.L. Perez-Ordoñez, I. Martinez-Lage, P. Vazquez-Burgo, Analytical and genetic programming model of compressive strength of eco-concretes by NDT according to curing temperature, *Constr. Build. Mater.* 144 (2017) 195–206, <https://doi.org/10.1016/j.conbuildmat.2017.03.123>.
- [32] R.H. Faraj, A.A. Mohammed, A. Mohammed, K.M. Omer, H.U. Ahmed, Systematic multiscale models to predict the compressive strength of self-compacting concretes modified with nanosilica at different curing ages, *Eng. Comput.* (2021) 1–24, <https://doi.org/10.1007/s00366-021-01385-9>.
- [33] H.U. Ahmed, A.S. Mohammed, A.A. Mohammed, R.H. Faraj, Systematic multiscale models to predict the compressive strength of fly ash-based geopolymers concrete at various mixture proportions and curing regimes, *PLoS One* 16 (6) (2021), e0253006, <https://doi.org/10.1371/journal.pone.0253006>.
- [34] H.U. Ahmed, A.A. Abdalla, A.S. Mohammed, A.A. Mohammed, A. Mosavi, Statistical methods for modeling the compressive strength of geopolymers mortar, *Materials* 15 (2022) 1868, <https://doi.org/10.3390/ma15051868>.
- [35] A. Çevik, R. Alzebaree, G. Humur, A. Niş, M.E. Gülsan, Effect of nano-silica on the chemical durability and mechanical performance of fly ash based geopolymers concrete, *Ceram. Int.* 44 (11) (2018) 12253–12264, <https://doi.org/10.1016/j.ceramint.2018.04.009>.
- [36] D. Adak, M. Sarkar, S. Mandal, Structural performance of nano-silica modified fly-ash based geopolymers concrete, *Constr. Build. Mater.* 135 (2017) 430–439, <https://doi.org/10.1016/j.conbuildmat.2016.12.111>.
- [37] K. Behfarnia, M. Rostami, Effects of micro and nanoparticles of SiO₂ on the permeability of alkali activated slag concrete, *Constr. Build. Mater.* 131 (2017) 205–213, <https://doi.org/10.1016/j.conbuildmat.2016.11.070>.
- [38] P. Nuaklong, P. Jongvivatsakul, T. Pothisiri, V. Sata, P. Chindaprasirt, Influence of rice husk ash on mechanical properties and fire resistance of recycled aggregate high-calcium fly ash geopolymers concrete, *J. Clean. Prod.* 252 (2020), 119797, <https://doi.org/10.1016/j.jclepro.2019.119797>.
- [39] Y. Patel, I.N. Patel, M.J. Shah, Experimental investigation on compressive strength and durability properties of geopolymers concrete incorporating with nano-silica, *Int. J. Civ. Eng. Technol.* 6 (5) (2015) 135–143.
- [40] M. Ibrahim, M.A.M. Johari, M. Maslehdin, M.K. Rahman, Influence of nano-SiO₂ on the strength and microstructure of natural pozzolan based alkali activated concrete, *Constr. Build. Mater.* 173 (2018) 573–585, <https://doi.org/10.1016/j.conbuildmat.2018.04.051>.
- [41] B. Mahboubi, Z. Guo, H. Wu, Evaluation of durability behavior of geopolymers concrete containing Nano-silica and Nano-clay additives in acidic media, *J. Civ. Eng. Mater. Appl.* 3 (3) (2019) 163–171, <https://doi.org/10.22034/JCEMA.2019.95839>.
- [42] S. Naskar, A.K. Chakraborty, Effect of nano materials in geopolymers concrete, *Perspect. Sci.* 8 (2016) 273–275, <https://doi.org/10.1016/j.pisc.2016.04.049>.
- [43] P. Nuaklong, V. Sata, A. Wongsa, K. Srinavip, P. Chindaprasirt, Recycled aggregate high calcium fly ash geopolymers concrete with inclusion of OPC and nano-SiO₂, *Constr. Build. Mater.* 174 (2018) 244–252, <https://doi.org/10.1016/j.conbuildmat.2018.04.123>.
- [44] S. Vyas, S. Mohammad, S. Pal, N. Singh, Strength and durability performance of fly ash based geopolymers concrete using nano silica, *Int. J. Eng. Sci. Technol.* 4 (2) (2020) 1–12, <https://doi.org/10.29121/ijestv4.i2.2020.73>.
- [45] M. Etemadi, M. Pouraghajian, H. Gharavi, Investigating the effect of rubber powder and nano silica on the durability and strength characteristics of geopolymers concretes, *J. Civ. Eng. Mater. Appl.* 4 (4) (2020) 243–252, <https://doi.org/10.22034/jcema.2020.119979>.
- [46] G. Angelin Lincy, R. Velkennedy, Experimental optimization of metakaolin and nanosilica composite for geopolymers concrete paver blocks, *Struct. Concr.* (2020), <https://doi.org/10.1002/suco.201900555>.
- [47] M.C. Rocío, R.S. Williams, P. Alivisatos (Eds.), *Nanotechnology Research Directions: IWGN Workshop Report: Vision for Nanotechnology in the Next Decade*, Springer Science & Business Media, 2000.
- [48] M. Ibrahim, M.A.M. Johari, M.K. Rahman, M. Maslehdin, H.D. Mohamed, Enhancing the engineering properties and microstructure of room temperature cured alkali activated natural pozzolan based concrete utilizing nanosilica, *Constr. Build. Mater.* 189 (2018) 352–365, <https://doi.org/10.1016/j.conbuildmat.2018.08.166>.
- [49] J.M. Their, M. Özakça, Developing geopolymers concrete by using cold-bonded fly ash aggregate, nano-silica, and steel fiber, *Constr. Build. Mater.* 180 (2018) 12–22, <https://doi.org/10.1016/j.conbuildmat.2018.05.274>.
- [50] M. Ibrahim, M.K. Rahman, M.A.M. Johari, M. Maslehdin, Effect of incorporating nano-silica on the strength of natural pozzolan-based alkali-activated concrete, in: *Proceedings of the International Congress on Polymers in Concrete*, Springer, Cham, 2018, pp. 703–709. (https://doi.org/10.1007/978-3-319-78175-4_90).
- [51] A.M. Janaki, G. Shafabakhsh, A. Hassani, Laboratory evaluation of alkali-activated slag concrete pavement containing silica fume and carbon nanotubes, *Eng. J.* 25 (5) (2021) 21–31, <https://doi.org/10.4186/ej.2021.25.5.21>.
- [52] A. Carriço, J.A. Bogas, A. Hawren, M. Guedes, Durability of multi-walled carbon nanotube reinforced concrete, *Constr. Build. Mater.* 164 (2018) 121–133, <https://doi.org/10.1016/j.conbuildmat.2017.12.221>.
- [53] P. Jittabut, S. Horpibulsuk, Physical and microstructure properties of geopolymers nanocomposite reinforced with carbon nanotubes, *Mater. Today Proc.* 17 (2019) 1682–1692, <https://doi.org/10.1016/j.matpr.2019.06.199>.
- [54] G. da Luz, P.J.P. Gleize, E.R. Batiston, F. Pelisser, Effect of pristine and functionalized carbon nanotubes on microstructural, rheological, and mechanical behaviors of metakaolin-based geopolymers, *Cem. Concr. Compos.* 104 (2019), 103332, <https://doi.org/10.1016/j.cemconcomp.2019.05.015>.
- [55] H.M.M. Khater, *Physicomical properties of nano-silica effect on geopolymers composites*, *J. Build. Mater. Struct.* 3 (1) (2016) 1–14.
- [56] A. Mohammed, W. Mahmood, K. Ghafor, TGA, rheological properties with maximum shear stress and compressive strength of cement-based grout modified with polycarboxylate polymers, *Constr. Build. Mater.* 235 (2020), 117534, <https://doi.org/10.1016/j.conbuildmat.2019.117534>.
- [57] A. Mohammed, S. Rafiq, P. Sihag, R. Kurda, W. Mahmood, Soft computing techniques: systematic multiscale models to predict the compressive strength of HVFA concrete based on mix proportions and curing times, *J. Build. Eng.* 33 (2021), 101851, <https://doi.org/10.1016/j.jobe.2020.101851>.
- [58] P. Sihag, P. Jain, M. Kumar, Modelling of impact of water quality on recharging rate of storm water filter system using various kernel function based regression, *Model. Earth Syst. Environ.* 4 (1) (2018) 61–68, <https://doi.org/10.1007/s40808-017-0410-0>.
- [59] E. Demircan, S. Harendra, C. Vipulanandan, Artificial neural network and nonlinear models for gelling time and maximum curing temperature rise in polymer grouts, *J. Mater. Civ. Eng.* 23 (4) (2011) 372–377, [https://doi.org/10.1061/\(ASCE\)MT.1943-5533.0000172](https://doi.org/10.1061/(ASCE)MT.1943-5533.0000172).
- [60] J. Quinlan Ross, Learning with continuous classes, in: *Proceedings of the 5th Australian Joint Conference on Artificial Intelligence*, Singapore, 1992, pp. 343–348.
- [61] D. Malerba, F. Esposito, M. Ceci, A. Appice, Top-down induction of model trees with regression and splitting nodes, *IEEE Trans. Pattern Anal. Mach. Intell.* 26 (5) (2004) 612–625, <https://doi.org/10.1109/TPAMI.2004.1273937>.
- [62] A.S. Mohammed, Vipulanandan models to predict the electrical resistivity, rheological properties and compressive stress-strain behavior of oil well cement modified with silica nanoparticles, *Egypt. J. Pet.* 27 (4) (2018) 1265–1273, <https://doi.org/10.1016/j.ejpe.2018.07.001>.
- [63] N. Hamed, M.S. El-Feky, M. Kohail, E.S.A. Nasr, Effect of nano-clay de-agglomeration on mechanical properties of concrete, *Constr. Build. Mater.* 205 (2019) 245–256, <https://doi.org/10.1016/j.conbuildmat.2019.02.018>.
- [64] D. Hardjito, S.E. Wallah, D.M. Sumajouw, B.V. Rangan, On the development of fly ash-based geopolymers concrete, *Mater. J.* 101 (6) (2004) 467–472.
- [65] P.S. Deb, P. Nath, P.K. Sarker, The effects of ground granulated blast-furnace slag blending with fly ash and activator content on the workability and strength properties of geopolymers concrete cured at ambient temperature, *Mater. Des.* 62 (1980–2015) (2014) 32–39, <https://doi.org/10.1016/j.matdes.2014.05.001>.
- [66] S. Oyebisi, A. Ede, F. Olutoge, D. Omole, Geopolymer concrete incorporating agro-industrial wastes: Effects on mechanical properties, microstructural behaviour and mineralogical phases, *Constr. Build. Mater.* 256 (2020), 119390, <https://doi.org/10.1016/j.conbuildmat.2020.119390>.

- [67] A.A. Aliabdo, M. Abd Elmoaty, H.A. Salem, Effect of water addition, plasticizer and alkaline solution constitution on fly ash based geopolymers concrete performance, *Constr. Build. Mater.* 121 (2016) 694–703, <https://doi.org/10.1016/j.conbuildmat.2016.06.062>.
- [68] M.T. Ghafoor, Q.S. Khan, A.U. Qazi, M.N. Sheikh, M.N.S. Hadi, Influence of alkaline activators on the mechanical properties of fly ash based geopolymers cured at ambient temperature, *Constr. Build. Mater.* 273 (2021), 121752, <https://doi.org/10.1016/j.conbuildmat.2020.121752>.
- [69] A. Hassan, M. Arif, M. Shariq, Effect of curing condition on the mechanical properties of fly ash-based geopolymers concrete, *SN Appl. Sci.* 1 (12) (2019) 1–9, <https://doi.org/10.1007/s42452-019-1774-8>.